GAS FLOW DURING WELL TESTING

A REPORT SUBMITTED TO THE DEPARTMENT OF PETROLEUM ENGINEERING

OF STANFORD UNIVERSITY

IN PARTIAL FULFILLMENT OF THE REQUIREMENTS FOR THE DEGREE OF MASTER OF SCIENCE

By

Zhun Li

June 2006

I certify that I have read this report and that in my opinion it is fully adequate, in scope and in quality, as partial fulfillment of the degree of Master of Science in Petroleum Engineering.

_____

Roland N. Horne
(Principal Advisor)

Abstract

The methods of gas well testing may be different from those of liquid well testing due to the nonlinearity of the gas flow equation. The pseudopressure, pseudotime and material balance pseudotime methods are three of the analytical methods used in gas well testing. These three methods resolve the nonlinearity of the gas flow equation by making transformations and assumptions to linearinze the gas flow equation approximately. However, these three methods do not always work. The objective of this research was to investigate under which conditions these methods work or not.

In this research, the simulation method was assumed to be accurate and be treated as "true data" and was used to provide a "benchmark" to evaluate the accuracies of these three analytical methods. Several cases were designed to study the validity of the three analytical methods. For each case the results of the pseudopressure, pseudotime and material balance pseudotime methods were compared with that of simulation. Some conclusions were drawn on the basis of these case studies.

For all the cases, three kinds of well test schemes were studied, namely drawdown tests during pseudosteady state, buildup tests with the well shut in during infinite-acting radial flow period and buildup test with the well shut in during pseudosteady state.

Acknowledgments

I wish to express my sincere appreciation to Prof. Roland N. Horne for his advice and support throughout the course of this work.

Thanks also to the faculty, staff and students of the Department of Petroleum Engineering, especially Masahiko Nomura, Chunmei Shi, Isha Sahni, Olubusola Tomas, Yaqing Fan, Qing Chen, Yuanlin Jiang and Egill Juliusson.

I also thank the Well Testing Group of Stanford University Petroleum Research Institute (SUPRI-D) for providing the financial support that made this work possible.

I would also like to thank Schlumberger for making the reservoir simulator Eclipse available for the study.

Lastly I would like to thank my parents for supporting and encouraging me always.

Contents

List of Tables

List of Figures

Chapter 1

1. Introduction

The ability to analyze the performance and forecast the production of gas wells is important in gas reservoir engineering. To obtain a reasonable degree of accuracy, different analytical methods have been studied and applied to modern gas well testing. Many of them were developed with the intent of linearizing the nonlinear gas flow equation. However, with modern computers we could solve the fully nonlinear gas flow equations completely, instead of making approximate linearizations. What would be the advantages or disadvantages in doing so?

1.1. Aims of this Research

Compared with the governing equation for liquid flow, the gas flow equation is nonlinear. Currently we can not obtain a fully analytical solution for the nonlinear gas flow equation. In gas well testing, the gas flow solution is obtained by transforming the governing equation into an approximately linear form which is similar to the liquid flow equation. Hence the solutions originally used for liquid flow can then be used to describe the gas flow. Several analytical methods have been introduced to approximately linearize the gas flow equation, but the approaches are different. Among these methods, three of them are the most important, namely the pseudopressure method, pseudotime method and material balance pseudotime method. Since linear approximations were used when applying these methods, for conditions under which these approximations do not fully apply, these methods will sometimes be inaccurate. One example is the long term drawdown test. If the whole reservoir pressure drops significantly, the pseudopressure method will not work. The aim of this study was to identify the conditions under which these methods are accurate or not.

With the help of modern computers, we could solve the nonlinear gas flow equations completely with a numerical approach such as simulation. Theoretically, by carefully adjusting the griding level of the simulation, one can approach a degree of accuracy that is high enough for well testing. Based on this theory, one of the basic ideas of this study was that the simulation method is accurate and can be used as the "true data". Simulation was used in this study to provide a "benchmark" for the three analytical methods. For each case designed in this study, the results of all the three analytical methods were compared with the "data" obtained from simulation. By doing so, the applicability and accuracy of each of these analytical methods was investigated.

No analytical method can describe the reservoir gas flow accurately. Every analytical method uses approximation and has limitation. The aim of this research was to find out under which conditions the pseudopressure, pseudotime and material balance pseudotime method will work or not.

1.2. Reservoir Model

In this work, only single-phase gas flow was studied. The porous medium was considered to be incompressible. The reservoir model was considered to be a closed boundary circular reservoir with a single production well at the center. The gravitational effect was neglected. Hence the gas flow can be treated as two-dimensional radial flow. A table of dry gas PVT properties was generated using a standard correction. This PVT table was used in all the cases in this study.

1.3. Period of Investigation

Both pressure drawdown tests and drawdown-buildup tests were studied. The infinite-acting radial flow and pseudosteady state flow were both investigated. For pressure drawdown tests, the two flow periods were studied by comparing their behavior. For drawdown-buildup tests, two cases were studied. In one case the producing well was shut in at the end of infinite-acting radial flow. In the other case, the producing well was shut in during pseudosteady state.

1.4. Case Studies

To investigate the main factors that could affect the accuracy of these three analytical methods, different cases were built. Three potential factors were studied, namely initial reservoir pressure, reservoir permeability and production rate. Only constant production rate tests were considered in this study.

Chapter 2

2. Theory

This chapter presents the equations and formulations used to generate the three analytical methods. Sections 2.1 and 2.2 discuss the general liquid and gas flow equation, and the three analytical methods that were used, namely pseudopressure, pseudotime and material balance time.

2.1. Equation of Liquid Flow

The derivation of the liquid flow differential equation assumes that Darcy's law is valid. Combining Darcy's law and the equation of continuity leads to a linear differential equation. Equation (2.1) is Darcy's law for horizontal flow, Equation (2.2) is the equation of continuity.

Darcy's Law for Horizontal Flow:

$$\vec{u} = -\frac{k}{\mu}\nabla p \tag{2.1}$$

Equation of Continuity:

$$\nabla(\rho\vec{v}) = -\frac{\partial}{\partial t}(\rho\phi) \tag{2.2}$$

In addition to Equation (2.1) and (2.2), the following assumptions (a)-(e) are also made:

(a) Constant porosity, ϕ.

(b) Constant and isotropic homogeneous permeability, k.

(c) Isothermal flow.

(d) No gravitational effect (assumed in Equation (2.1)).

(e) Incompressible porous media.

Using these equations and assumptions, the liquid flow equation can be obtained as in Equation (2.3):

$$\frac{1}{r}\frac{\partial}{\partial r}(r\frac{\partial p}{\partial r}) = \frac{\phi \mu c}{k}\frac{\partial p}{\partial t} \tag{2.3}$$

By assuming constant compressibility and viscosity, Equation (2.3) can be treated as a linear diffusion equation. A solution set has been developed for the dimensionless diffusion equation. Then the final solution can be obtained by transforming the dimensionless variables into dimensional form.

2.2. Equation of Gas Flow

In addition to assuming the validity of Darcy's law, the gas flow equation also assumes that the real gas equation of state applies. Combining the equation of state, Darcy's law and the equation of continuity results in a nonlinear differential equation. Equation (2.4) is Darcy's law for horizontal flow, Equation (2.5) is the equation of continuity, Equation (2.6) is the gas equation of state.

Darcy's Law for Horizontal Flow:

$$\vec{u} = -\frac{k}{\mu}\nabla p \tag{2.4}$$

Equation of Continuity:

$$\nabla(\rho\vec{v}) = -\frac{\partial}{\partial t}(\rho\phi) \tag{2.5}$$

Equation of State:

$$\rho = \frac{pM}{zRT} \tag{2.6}$$

In addition to these three equations, assumptions (a) to (e) in Section 2.1 are also applied. The general gas flow equation is obtained by combining Equation (2.4), (2.5), (2.6) and assumptions (a) to (e):

$$\frac{\partial}{\partial t}(\frac{p}{z}) = \frac{k}{\phi}\nabla[\frac{p}{\mu z}\nabla p] \tag{2.7}$$

Unlike the liquid flow equation, the gas flow equation is nonlinear. Currently there is no analytical solution to this equation. Equation (2.7) has to be transformed to an approximately linear form to obtain further solution.

2.3. Pseudopressure Method

Among the traditional analytical methods for gas well testing, the pseudopressure method is the most common. The concept of pseudopressure was introduced by Al-Hussainy et al. (1966). Equation (2.8) shows the definition of pseudopressure:

$$\varphi \equiv 2\int_{p^0}^{p} \frac{p}{\mu z} dp \tag{2.8}$$

Where p^0 is the reference pressure. In this work p^0 was specified as the initial reservoir pressure. Substituting Equation (2.8) into Equation (2.7) gives:

$$\frac{1}{r}\frac{\partial}{\partial r}(r\frac{\partial \varphi}{\partial r}) = \frac{\phi \mu c}{k}\frac{\partial \varphi}{\partial t} \tag{2.9}$$

Equation (2.9) is very similar to Equation (2.3), the linear equation of the liquid flow, except that the pressure variable is replaced by pseudopressure φ. If Equation (2.9) is considered to be linear, it can be solved by applying the solution of Equation (2.3).

Before solving the gas pseudopressure equation, a table or curve of $\varphi - p$ is constructed. Once the $\varphi - p$ conversion table is obtained, any pressure can be easily converted to φ and vice versa. Given the assumption of isothermal flow (assumption (c) in Section 2.1), which in most cases applies, the $\varphi - p$ table can be valid for the entire reservoir and the whole well testing period.

Pseudopressure φ only depends on the relation between μz and pressure. Whenever the PVT table of the gas is given, the $\varphi - p$ relation is definite. It should be noted that φ is independent of time. An example of a $\varphi - p$ curve is shown in Figure 2-1.

By considering the diffusivity term $\frac{\phi\mu c}{k}$ in Equation (2.7) to be constant, which in most short-term test cases applies, Equation (2.7) can be treated as a linear diffusion equation. In practice, this term is usually evaluated at the initial reservoir pressure p_i.

It is convenient to express the flow Equation (2.7) and the relevant boundary conditions in dimensionless terms as in Equation (2.10) (Energy Resources Conservation Board, Canada, 1979):

$$\frac{1}{r_D}\frac{\partial}{\partial r_D}(r_D\frac{\partial p_D}{\partial r_D}) = \frac{\partial}{\partial t_D}(\Delta p_D) \tag{2.10}$$

where the dimensionless terms Δp_D and t_D for radial-cylindrical flow are defined in Equations (2.11) and (2.12):

$$\Delta p_D = \frac{\varphi_i - \varphi}{\varphi_i q_D} \tag{2.11}$$

$$t_D = \frac{\lambda k t}{\phi \mu_i c_i r_w^2} \tag{2.12}$$

The definition of r_D and φ_i are shown in Equations (2.13) and (2.14):

$$r_D = \frac{r}{r_w} \tag{2.13}$$

$$q_D = \frac{\gamma T q}{k r \varphi_i} \tag{2.14}$$

where q is the gas production rate. λ and γ are the constants used for the dimensionless terms in field units. For radial-cylindrical flow, the values of these two coefficients are:

$\lambda = 2.637 \times 10^{-4}$

$\gamma = 1.422 \times 10^{6}$

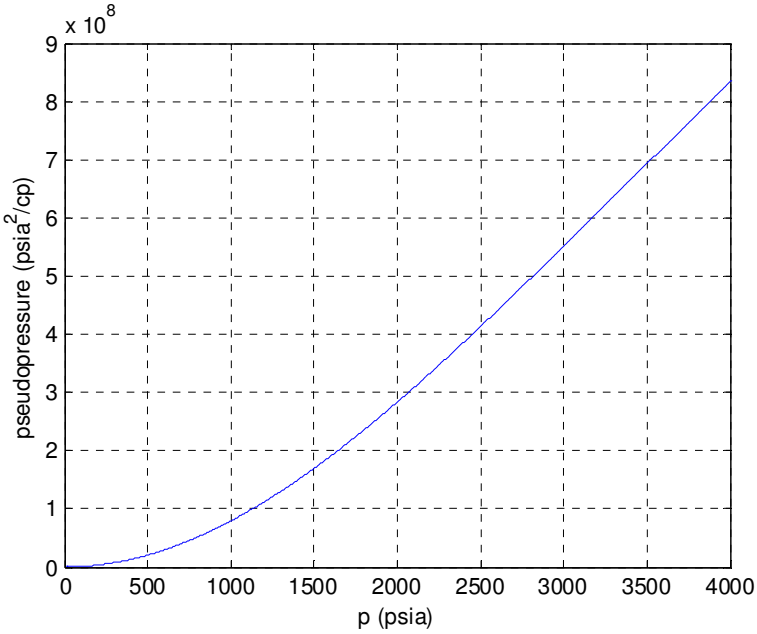

Figure 2-1: Example plot of pseudopressure vs. real pressure.

For the drawdown test with constant surface production rate, the solution for Equation (2.10) at the well is shown in Equation (2.15) (Energy Resources Conservation Board, Canada, 1979):

$$p_t = \Delta p_D \mid_{well} = \begin{cases} -\frac{1}{2} Ei(-\frac{1}{4t_D}) & for\, t_D < 25 \\ \frac{1}{2}(\ln t_D + 0.809) & for\, t_D \geq 25 \\ \frac{2t_D}{r_{eD}^2} + \ln r_{eD} - \frac{3}{4} & for\, \frac{t_D}{r_{eD}^2} \geq 0.25 \end{cases} \tag{2.15}$$

The problem in this research is a forward modeling problem. Hence the approach in this research was to directly generate the p_t solution from Equation (2.15) for certain t_D. Then dimensional pseudopressure φ at the well could be obtained using Equation (2.11). Finally the wellbore pressure solution could be obtained by checking the $\varphi - p$ table.

It should be noted that the solution in Equation (2.15) is valid only when the diffusivity term $\frac{\phi\mu c}{k}$ is approximagely constant. When this assumption does not apply, the solution in Equation (2.15) will not be valid.

An example is the long term drawdown test. For a closed boundary reservoir, when the boundary flow is detected, the system will enter into pseudosteady state, and the average reservoir pressure will drop. In this case, the diffusivity term $\frac{\phi\mu c}{k}$ may drop significantly and the solution in Equation (2.15) would not apply.

Figure 2-2 shows an example of short term drawdown test in which the pseudopressure method works. In this example, the flow period was limited to infinite-acting radial flow. The example used the same gas PVT property that was used to construct the $\varphi - p$ table in Figure 2-1, which means that the same $\varphi - p$ relation could be applied. In Figure 2-2, the result of the pseudopressure method matches the Eclipse "data".

Figure 2-3 shows an example of a long term drawdown test in which the pseudopressure method does not work. The same $\varphi - p$ curve was used. The production was much longer so the average reservoir pressure was allowed to drop significantly. In Figure 2-3 there is a big deviation between the pseudopressure solution and the Eclipse "data". The reason for the inaccuracy of pseudopressure method, as mentioned previously, is the drop of the diffusivity term $\frac{\phi\mu c}{k}$ due to the significant drop of reservoir pressure.

To deal with the nonlinearity of the diffusivity term, another transformation, the pseudotime method, has been introduced.

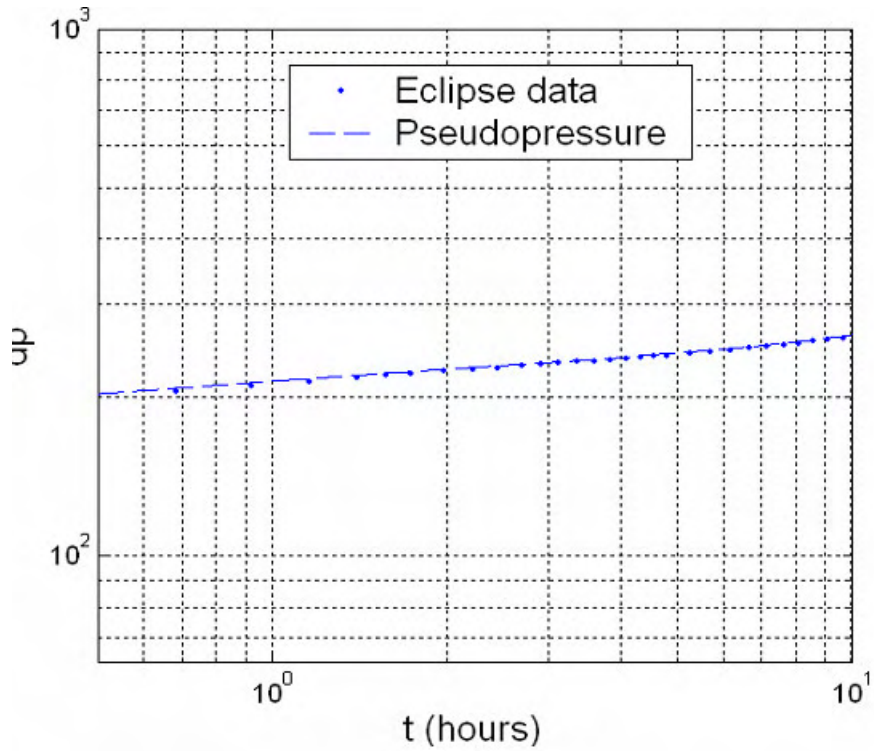

Figure 2-2: Example of the pseudopressure method used in a drawdown test during infinite-acting radial flow.

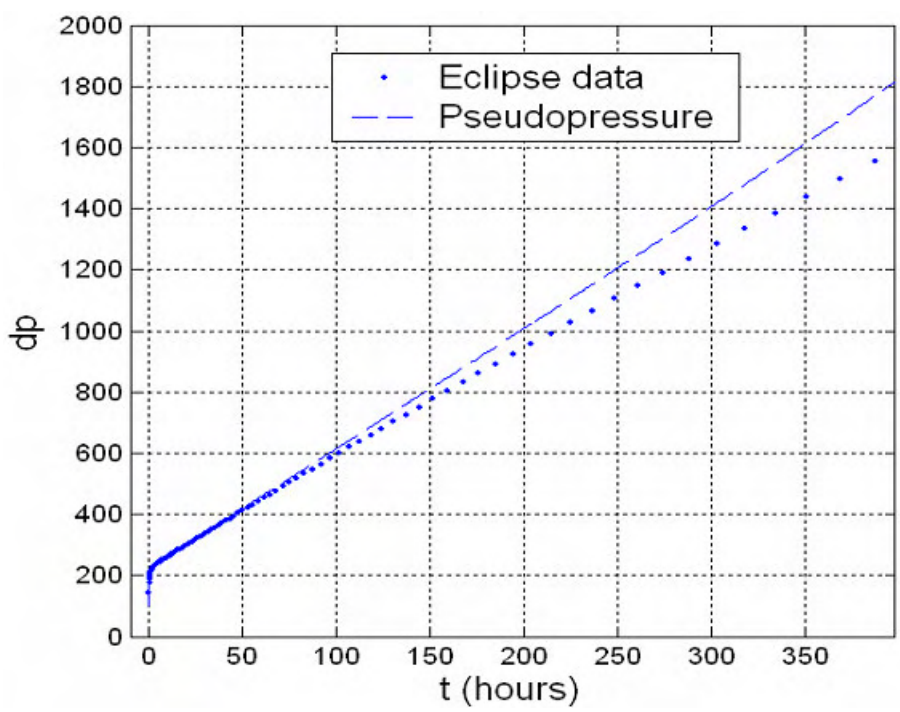

Figure 2-3: Example of the pseudopressure method in a long term test.

2.4. Pseudotime Method

The concept of pseudotime was introduced by Agarwal (1979) and its use developed by Lee and Holditch (1982). The definition of pseudotime is given in Equation (2.16):

$$t_a \equiv \int_p^t \frac{dt}{\mu c} \tag{2.16}$$

By substituting the Equation (2.16) into Equation (2.9) one can obtain the gas flow equation in term of both pseudopressure and pseudotime, which is shown in Equation (2.17):

$$\frac{1}{r}\frac{\partial}{\partial r}(r\frac{\partial \varphi}{\partial r}) = \frac{\phi}{k}\frac{\partial \varphi}{\partial t_a} \tag{2.17}$$

After dimensionless transformation, Equation (2.17) can be expressed as:

$$\frac{1}{r_D}\frac{\partial}{\partial r_D}(r_D\frac{\partial \varphi_D}{\partial r_D}) = \frac{\partial \varphi_D}{\partial t_{aD}} \tag{2.18}$$

Where t_{aD} is dimensionless pseudotime and is defined as:

$$t_{aD} = \frac{\lambda k t_a}{\phi r_w^2} \tag{2.19}$$

Without wellbore storage, the inner boundary condition of the pseudotime method will be the same as the pseudopressure method (Lee and Holditch, 1982).

Compared with Equation (2.9), the diffusivity term in Equation (2.17) consists of only permeability k and porosity ϕ. By assuming permeability k and porosity ϕ constant and isotropic, which is valid in most cases for well testing, the gas flow equation in term of pseudotime will be completely linear. The nonlinearity that is unsolved in the pseudopressure method now is resolved by applying the pseudotime method.

In this work, Equation (2.18) was solved first and a relation between dimensionless pseudopressure and dimensionless pseudotime was obtained. Since Equation (2.18) has exactly the same form as Equation (2.10), the solution in Equation (2.15) can be applied to solve Equation (2.18). Then the pressure and time could be computed from

dimensionless pseudopressure and pseudotime by applying the dimensional transform. The final step was to calculate real pressure from pseudopressure and real time from pseudotime.

It is straightforward to calculate real pressure from pseudopressure by checking the $\varphi - p$ table. However, to calculate time t from pseudotime t_a is more complex. Traditional well testing is an inverse problem. For the inverse problem, the wellbore pressure as a function of time is the input. By applying Equations (2.8) and (2.16), pseudopressure and pseudotime can be obtained very straightforwardly using numerical integration such as the method provided by Agarwal (1979). But this is not the case in this research because this work is a forward modeling problem and time should be calculated from pseudotime. In this work, an inverse trapezoidal method was used to obtain real time from pseudotime.

Suppose that time steps are chosen to be small enough that Equation (2.16) can be evaluated using trapezoidal integration. Figure 2-4 shows how the pseudotime can be calculated using trapezoidal integration. $\frac{1}{\mu c}$ is a function of pressure, hence it is also a function of time and is plotted versus t in Figure 2-4. By the definition of Equation (2.16), the area under the $\frac{1}{\mu c} - t$ curve is pseudotime. For example, in Figure 2-4, the area of the shaded part is the pseudotime corresponding to t_3.

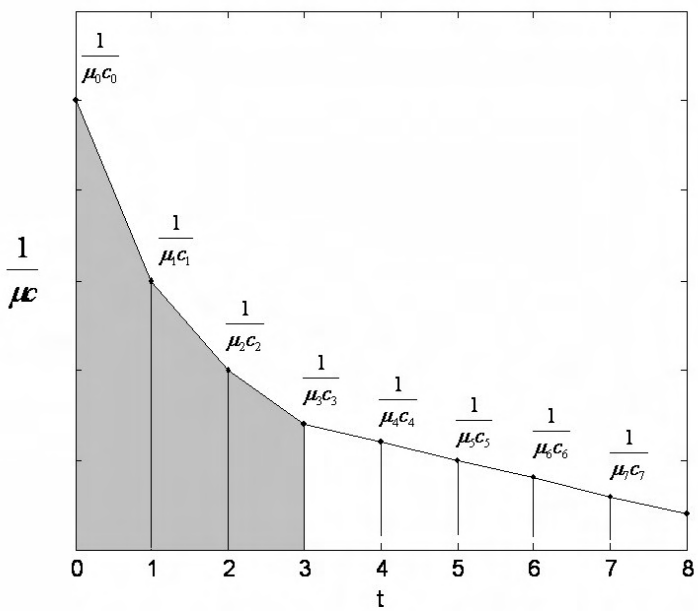

Figure 2-4: Pseudotime can be calculated using trapezoidal integration. By the definition of pseudotime, the area of the shaded part is the pseudotime value corresponding to t_3.

Defining t_{a0}, t_{a1} and t_{a2} as the pseudotime corresponding to the real t_0, t_1 and t_2 and so on, and applying the trapezoidal rule, we have:

$$\begin{cases} t_{a0} = 0 \\ t_{a1} = \frac{1}{2}(t_1 - t_0)(\frac{1}{\mu_0 c_0} + \frac{1}{\mu_1 c_1}) + t_{a0} \\ t_{a2} = \frac{1}{2}(t_2 - t_2)(\frac{1}{\mu_1 c_1} + \frac{1}{\mu_2 c_2}) + t_{a1} \\ t_{a3} = \frac{1}{2}(t_3 - t_2)(\frac{1}{\mu_2 c_2} + \frac{1}{\mu_3 c_3}) + t_{a0} \\ ..... \end{cases} \tag{2.20}$$

By rewriting Equation (2.20), Equation (2.21) can be obtained:

$$
\begin{cases}
t_0 = 0 \\
t_1 = \dfrac{2(t_{a1} - t_{a0})}{\dfrac{1}{\mu_0 c_0} + \dfrac{1}{\mu_1 c_1}} + t_0 \\
t_2 = \dfrac{2(t_{a2} - t_{a1})}{\dfrac{1}{\mu_1 c_1} + \dfrac{1}{\mu_2 c_2}} + t_1 \\
t_3 = \dfrac{2(t_{a3} - t_{a2})}{\dfrac{1}{\mu_2 c_2} + \dfrac{1}{\mu_3 c_3}} + t_2 \\
\ldots\ldots
\end{cases}
\tag{2.21}
$$

In Equation (2.21), $\frac{1}{\mu c}$ is a function of pseudopressure. Every pseudopressure corresponds to a pseudotime t_a. So $\frac{1}{\mu c}$ is a function of pseudotime and can be easily obtained. Then the real time t can be calculated using Equation (2.21).

An example of the application of pseudotime method is shown in Figure 2-5. This is the same long term drawdown case used in Section 2.4. In Figure 2-5 there are three curves plotted. These curves are the Eclipse "data", the results of the pseudopressure method and pseudotime method. The pseudotime method shows a good match with the Eclipse "data", compared to the bad prediction of pseudopressure method. In this case, the pseudotime transformation effectively linearizes the nonlinear gas flow equation and has improved the accuracy.

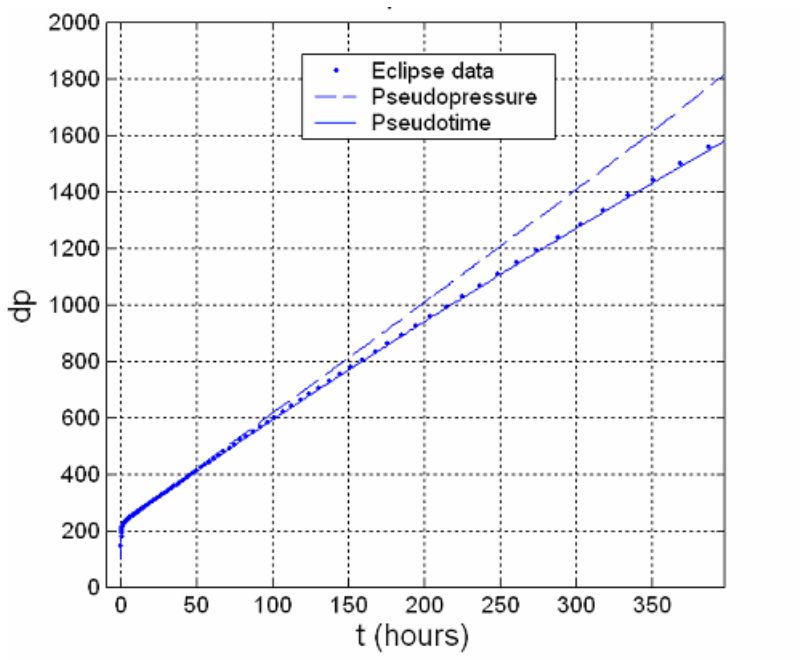

Figure 2-5: An example of the applicatioin of the pseudotime method. In this figure, the pseudotime method matches the Eclipse "data".

But the pseudotime method is not perfect. There are also conditions under which the pseudotime method does not work. An example is shown in Figure 2-6. This is also a long term drawdown test. These cases were built to study the reason why the pseudotime method does not work. Three potential factors that could influence the accuracy were investigated. These factors are initial reservoir pressure, reservoir permeability and surface production rate. The results of these cases will be provided and discussed in Chapter 3.

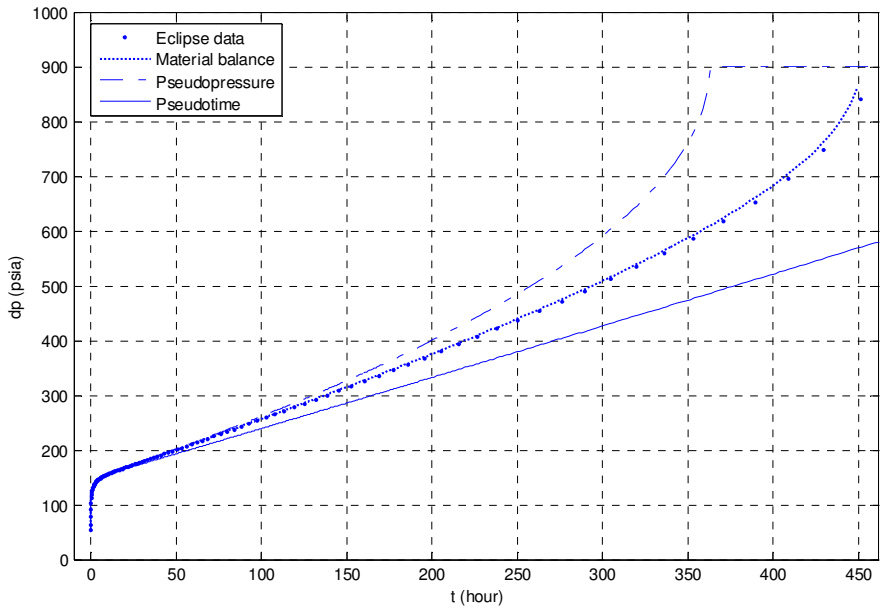

Figure 2-6: Example of the pseudotime method not matching.

2.5. Material Balance Pseudotime Method

The material balance pseudotime method is a variation of the pseudotime based method. The difference between these two methods is that in the pseudotime method, the pseudotime is evaluated at the wellbore pressure, while for material balance pseudotime method the pseudotime is evaluated at the average reservoir pressure.

The reason why this method is called material balance pseudotime method is that the average reservoir pressure is evaluated according to the material balance equation. The material balance equation was introduced by Ramagost and Farshad (1981) and is shown in Equation (2.22):

$$\frac{\overline{p}}{\overline{z}} = \frac{p_i}{z_i}[1 - \frac{G_p}{G}] \tag{2.22}$$

In Equation (2.22), $\overline{p}$ is average reservoir pressure, $\overline{z}$ is gas compressibility factor evaluated at $\overline{p}$. G_p is cumulative gas production, and can be calculated by integrating the

gas production rate over time. G is the original gas in place, and can be obtained by using Equation (2.23):

$$G = \frac{Ah\phi(1 - S_{wi})}{B_{gi}} \tag{2.23}$$

A $\frac{\overline{p}}{\overline{z}} - \overline{p}$ table was constructed using the PVT table. $\frac{\overline{p}}{\overline{z}}$ at every time point can be calculated by knowing both G_p and G. Hence, by checking the $\frac{\overline{p}}{\overline{z}} - \overline{p}$ table the average reservoir pressure $\overline{p}$ can be obtained.

Although the material balance pseudotime method is based on the pseudotime method, the basic procedures of these two algorithms are quite defferent. The algorithm used in the pseudotime method is much like a top-down procedure. The flowchart of the algorithm used in this work is shown in Figure 2-7. Firstly, the dimensionless equation was solved, which resulted in the dimensionless pseudopressure φ_D as a function of pseudotime t_{aD}. Then pseudopressure φ and pseudotime t_a were calculated from the dimensionless variables. By checking the $\varphi - p$ table, the pressure was obtained. Finally, real time t was calculated by knowing p as a function of t_a.

The algorithm of the material balance pseudotime method is different. The flowchart is shown in Figure 2-8. Instead of starting with solving the dimensionless equation, the material balance pseudotime method began with calculating the average reservoir pressure $\overline{p}$ at a certain time t. Applying Equation (2.21), the corresponding pseudotime t_a was calculated and the dimensionless pseudotime t_{aD} can be obtained. Then the dimensionless pseudopressure φ_D were obtained by solving the dimensionless equation. Finally the real pressure p can be obtained through checking the $\varphi - p$ table.

The trapezoidal method in Chapter 2.4 is quite complex and time expensive. Gardner et al. (2000) provided an analytical method that can calculate the pseudotime t_a from the average reservoir pressure $\overline{p}$ directly instead of making an integral. The flowchart of the

algorithm used in this work is shown in Figure 2-9. It should be noted that the difference between Figure 2-8 and Figure 2-9 is that in Figure 2-8 there are two inputs required to calculate t_a, but in Figure 2-9 only one input is needed. Both the trapezoidal integration based method and the analytical method have been investigated in this study. It was found that the results of the two methods were very close. To take advantage of the low CPU cost, the trapezoidal integration based method was used in all the case studies.

Since the material balance pseudotime method is a pseudotime based method, it is reasonable to assume that when the pseudotime method is accurate, material balance pseudotime method will also be accurate.

The same cases that were run for pseudotime method were also run for material balace pseudotime method. The results and discussions will be presented in Chapter 3.

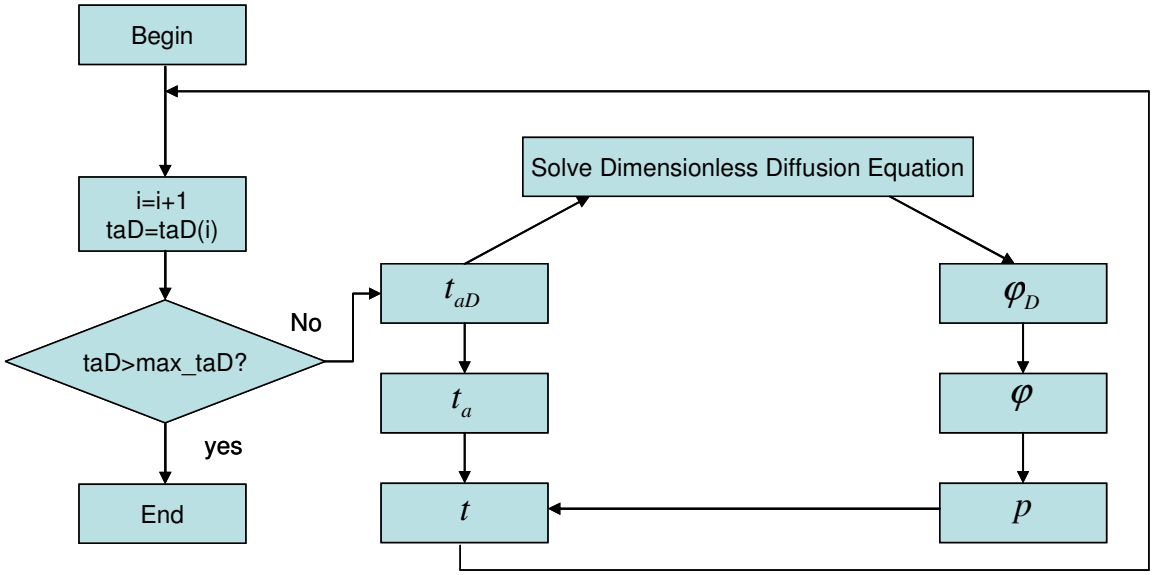

Figure 2-7: Flowchart of the pseudotime method used in this study.

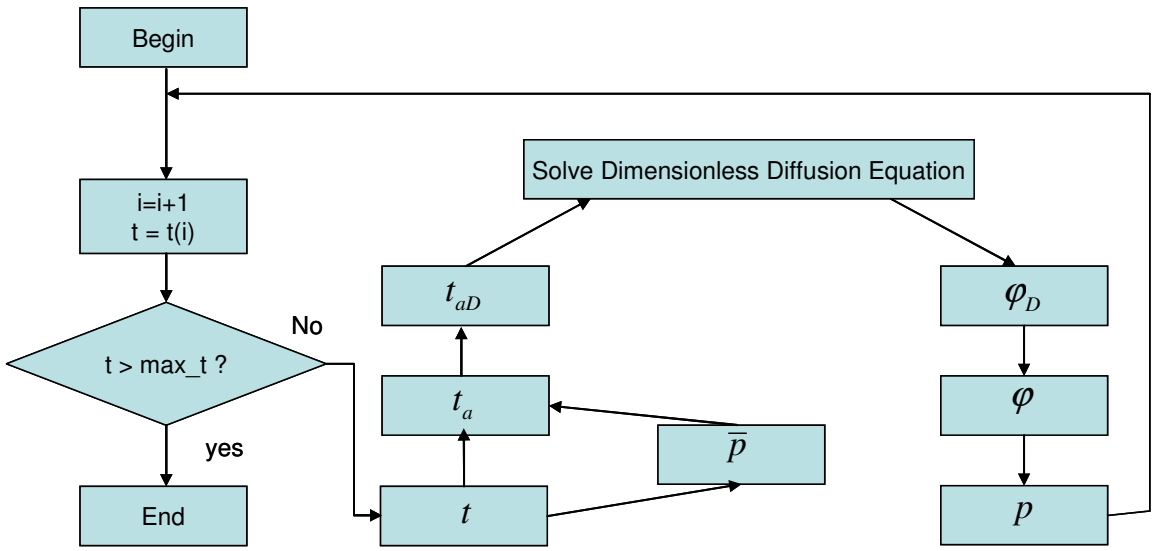

Figure 2-8: Flowchart of material balance pseudotime method that was used in this study with trapezoidal integration.

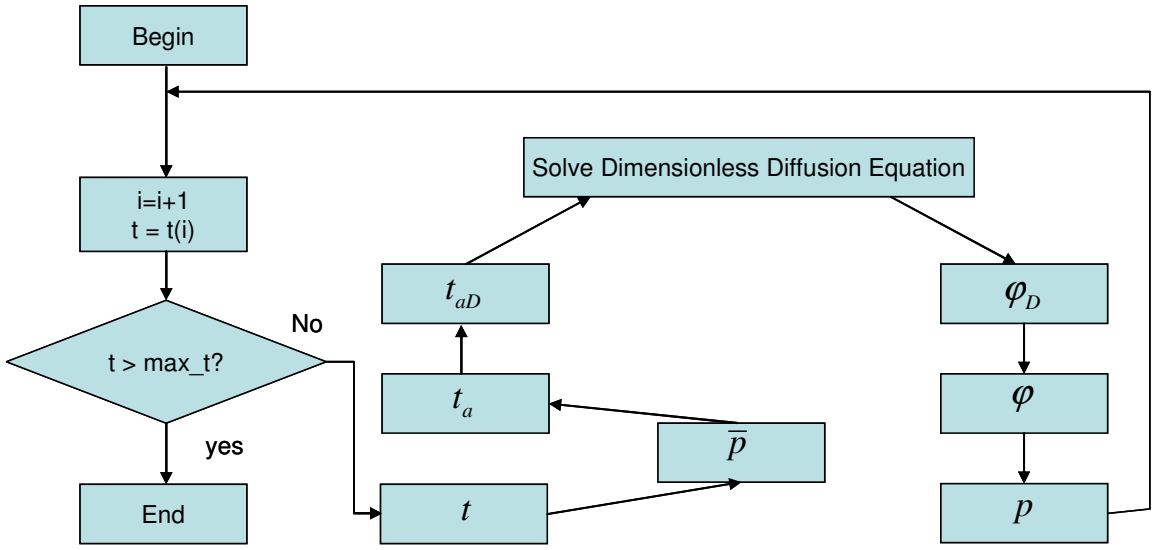

Figure 2-9: Flowchart of the material balance pseudotime method that was used in this study with the analytical approach.

2.6. Time Superposition in Buildup Tests

A buildup test involves the application of the principle of superposition. In this work the influence of time superposition to the three analytical methods was studied.

The principle of superposition can be applied when the differential equations and boundary conditions are linear. To apply time superposition, a typical buildup test can be treated as the combination of two flow rates, such as when q_B is q, starting at time zero, and q_C is $-q$, starting at the time t_p. The effect of the combination of these two flow rates is the same as the well being kept producing at a constant rate q and being shut in at time t_p (Figure 2-10) (Horne, 1995). Hence the solution can then be treated as a time superposition of these two flow rates (Figure 2-11). The solution function is shown in Equation (2.24).

$$p_D(t_D) = p_D(t_{pD} + \Delta t_D) - p_D(\Delta t_D) \tag{2.24}$$

For the pseudopressure method, a modification to Equation (2.24) should be made. This modification is shown in Equation (2.25):

$$\varphi_D(t_D) = \varphi_D^{'}(t_{pD} + \Delta t_D) - \varphi_D^{'}(\Delta t_D) \tag{2.25}$$

It should be noted that the gas flow equation in term of pseudopressure, which is shown in Equation (2.9), is not linear. Hence the time superposition described in Equation (2.25) is incomplete and it is questionable to apply the principle of superposition directly.

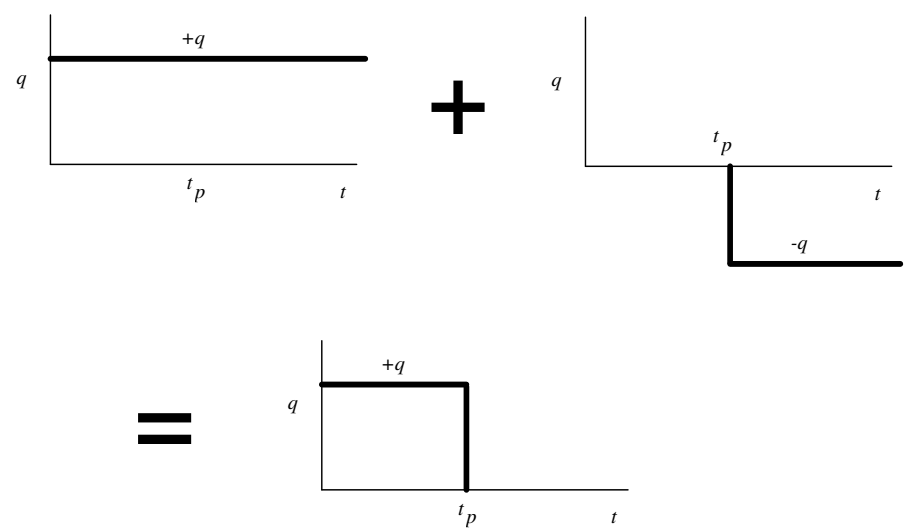

Figure 2-10: A well being kept producing and then shut in can be treated as the combination of two flow rates. This diagram is from Horne (1995).

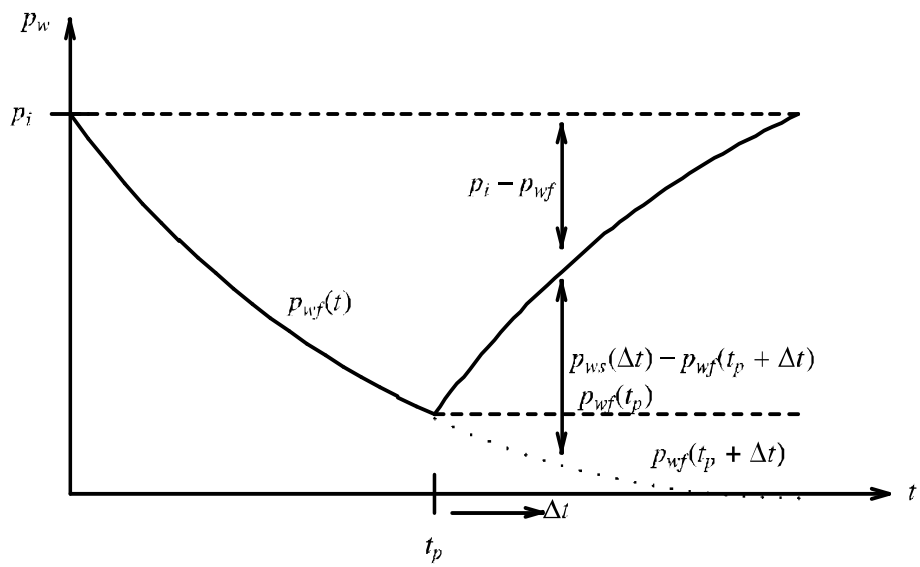

Figure 2-11: Illustration of the application of time superposition to a drawdown-buildup test. This diagram is from Horne (1995).

To apply the principle of superposition to the pseudotime method, another modification should be made and is shown in Equation (2.26).

$$\varphi_D(t_{aD}) = \varphi_D^{'}(t_{paD} + \Delta t_{aD}) - \varphi_D^{'}(\Delta t_{aD}) \tag{2.26}$$

where t_{paD} is the dimensionless pseudotime corresponding to t_p. Equation (2.26) is simple. However, it is very unintuitive to apply.

t_{aD} is a function of p and, accordingly, a function of φ_D. However, for the same Δt_{aD}, there are two φ_D functions on the right hand side of Equation (2.26). Adding the φ_D function on the left hand side of Equation (2.26), there will be three φ_D functions that can be used to evaluate t_{aD}. Which φ_D function should be picked to evaluate pseudotime?

In this study two approaches have been tried and the results compared. In the first approach the φ_D on the left hand side of Equation (2.26) was chosen. In the second approach both the two φ_D functions on the right hand side were picked and they were

added up in the time domain instead of in the pseudotime domain. In the following is a detailed discussion of these two approaches.

Approach 1: Evaluating t_{aD} at φ_D on the left hand side of Equation (2.26)

Making a modification on Equation (2.26) we can get:

$$\varphi_D(t_{aD}) = \varphi_D^{'}(t_{aD}) - \varphi_D^{'}(t_{aD} - t_{paD}) \tag{2.27}$$

For every pseudotime t_{aD}, $\varphi_D(t_{aD})$ was calculated by applying the solution of diffusion equation into Equation (2.27) directly. The real time t corresponding to t_{aD} was obtained and was evaluated at $\varphi_D(t_{aD})$. For this approach, every pseudotime point corresponded to a different time point. The flowcharts of this approach for the pseudotime method and the material balance pseudotime method are shown in Figure 2-12 and Figure 2-13.

Approach 2: Evaluating t_{aD} at φ_D on the right hand side of Equation (2.26)

This approach is much less intuitive compared with the previous one. The method also obeys Equation (2.27). However, each φ_D term on the right hand side of equation was first transformed into the time domain. Then these two φ_D functions were added up in the time domain. The basic idea of this approach is illustrated in Figure 2-14.

As Figure 2-14 shows, the first step is to generate solutions $\varphi_D^{'}(t_{aD})$ and $\varphi_D^{'}(t_{aD} - t_{paD})$. The second step is to transform these two solutions into the time domain. The third step is to add up the two new solutions in the time domain. It should be noted that for the same t_{aD}, two different t values may be obtained from $\varphi_D^{'}(t_{aD})$ and $\varphi_D^{'}(t_{aD} - t_{paD})$. This is because $\varphi_D^{'}(t_{aD})$ and $\varphi_D^{'}(t_{aD} - t_{paD})$ are different. As a function of pseudotime, the real time t values corresponding to $\varphi_D^{'}(t_{aD})$ and $\varphi_D^{'}(t_{aD} - t_{paD})$ will be different.

Neither of the two approaches makes a complete time superposition. Both these two approaches were tried and the results show that there is little difference between them.

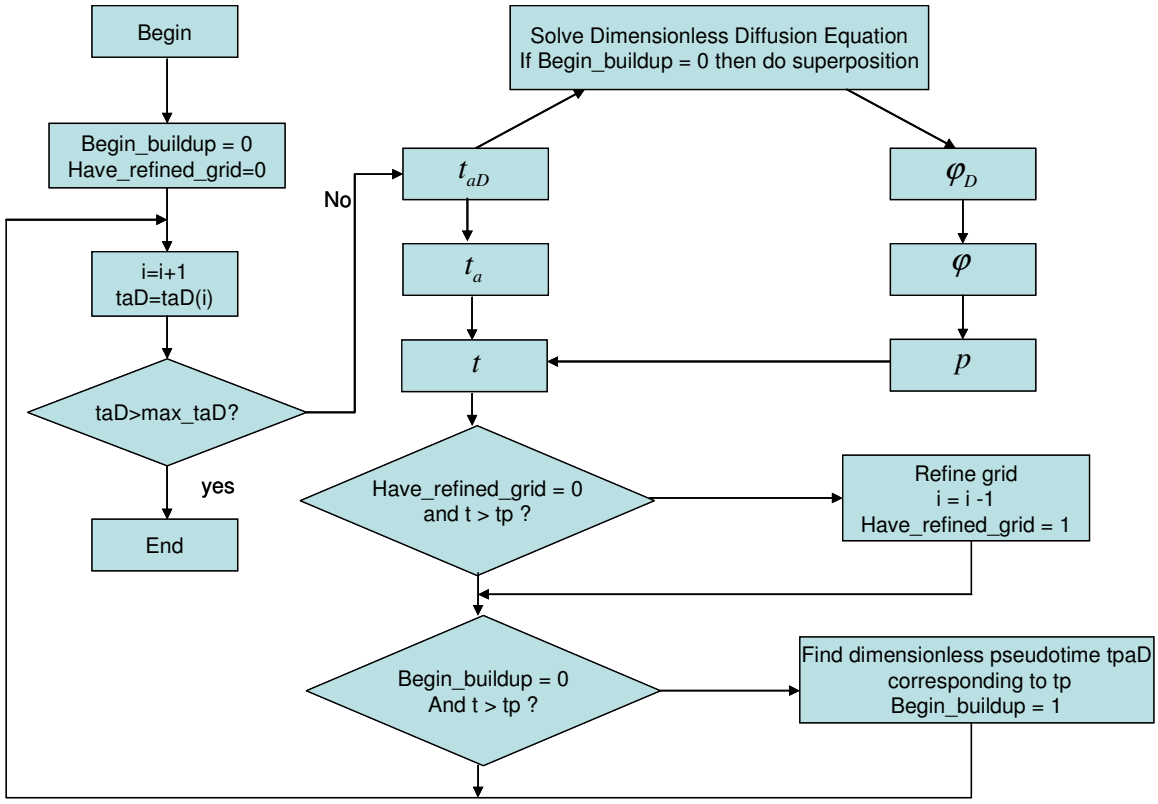

Figure 2-12: Flowchart of the pseudotime method with time superposition applied in buildup tests.

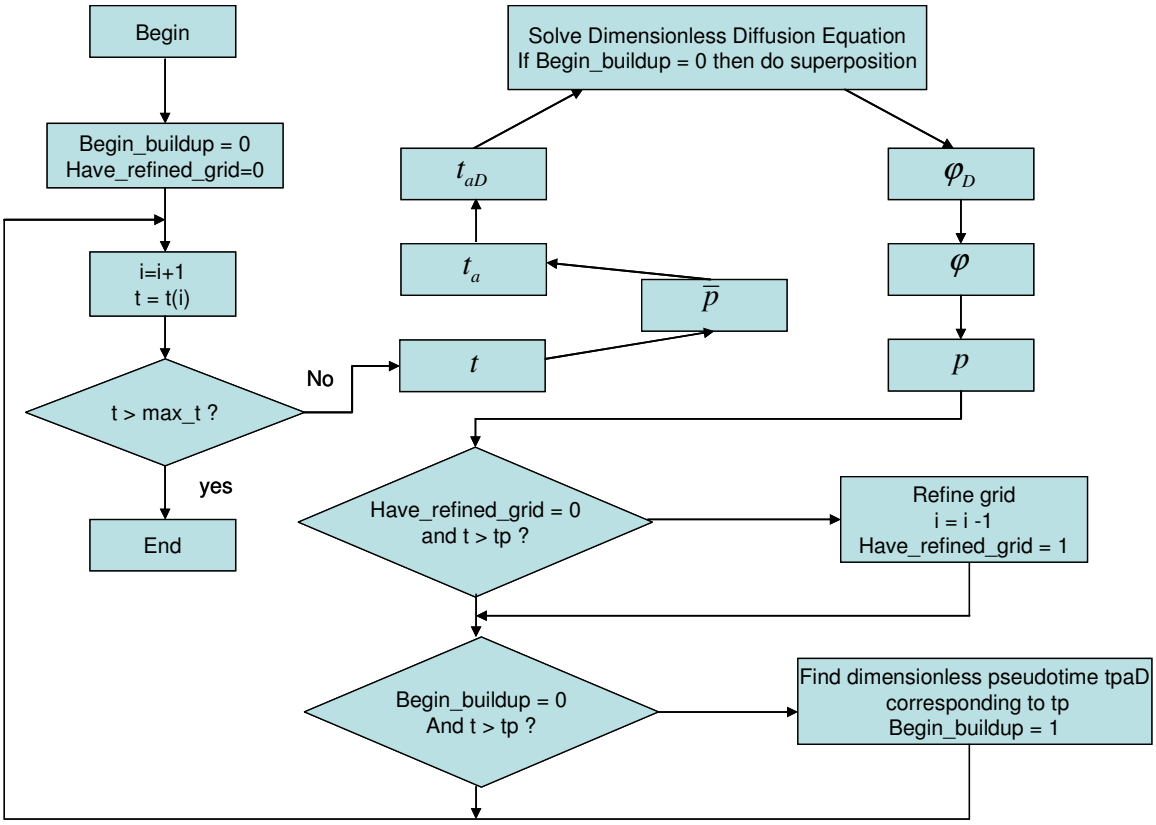

Figure 2-13: Flowchart of the material balance pseudotime method with time superposition applied to buildup tests.

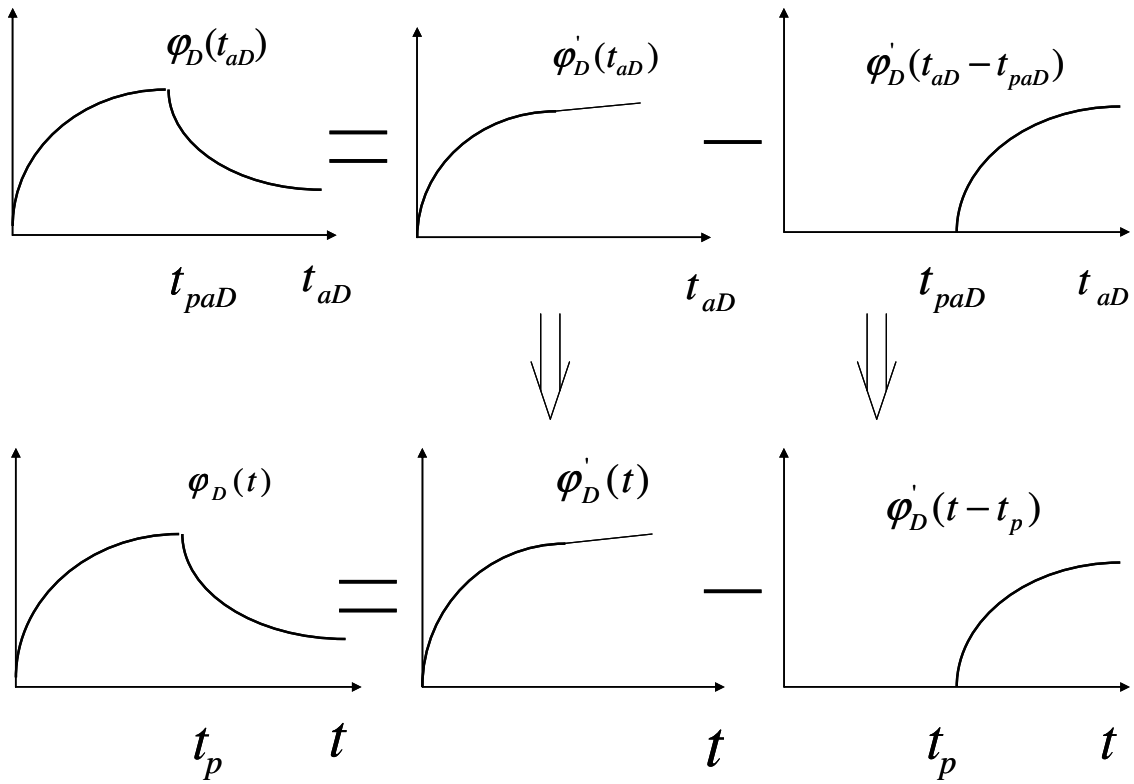

Figure 2-14: Illustration of the second approach of time superposition that was tried in this study. In this approach, $\varphi_D^{'}(t_{aD})$ and $\varphi_D^{'}(t_{aD}-t_{paD})$ were first generated and then transformed into the time domain. Finally $\varphi_D^{'}(t)$ and $\varphi_D^{'}(t-t_p)$ were added up in the time domain to obtain $\varphi_D(t)$.

Chapter 3

3. Results and Case Studies

This chapter presents the results of the case studies. These cases were run for all the three analytical methods, namely the pseudopressure method, pseudotime method and material balance pseudotime method. The results are discussed and some conclusions are drawn on the applicability of these methods.

3.1. Calculating Gas Properties

The gas properties were estimated using the method described by Horne (1995), Chapter 9. Gas formation volume factor B_g, viscosity μ, compressibility c and gas compressibility factor z were obtained.

The gas compositions used in this study are shown in Table 3-1. From Table 3-1, the average gas molecular weight was calculated to be 16.3562 $lb/lb-mole$ and specific gravity 0.5708. The reservoir temperature was set to be $200^{o}F$. It was assumed that there is no CO_2 and H_2S. The gas properties were estimated by treating the gas as California gas, and gas formation volume factor, viscosity, compressibility and z-factor vs. pressure were calculated. These parameters are plotted versus pressure in Figures 3-1, 3-2, 3-3 and 3-4.

By applying these gas properties, a $\varphi - p$ table can be constructed using Equation (2.8). Figure 3-5 shows the $\varphi - p$ plot. The gas properties obtained previously and the $\varphi - p$ table was applied to all the cases shown in this chapter.

Table 3-1: Gas compositions for estimating the gas PVT properties.

Compositions	Molecular percentage
C1	97.12
C2	2.42
C3	0.31
i-C4	0.05
n-C4	0.02
C6	0.02
C6+	0.06
Reservoir temperature:	200 Fahrenheit
Molecular weight:	16.5362 lb/lbmole
Specific gravity:	0.5708

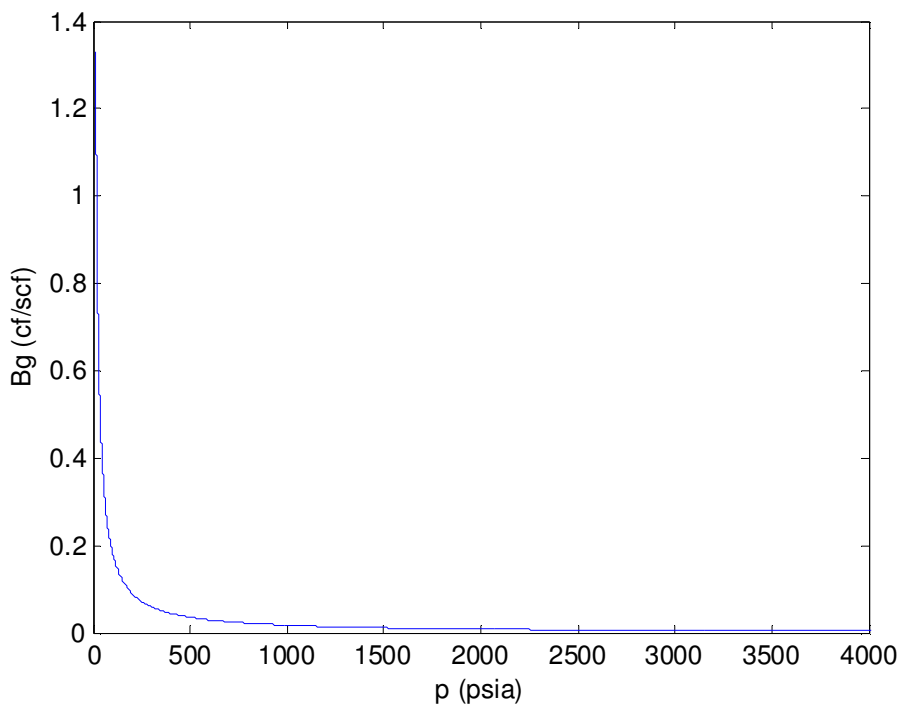

Figure 3-1: Plot of gas formation volume factor vs. pressure. It was applied to all the cases in this study.

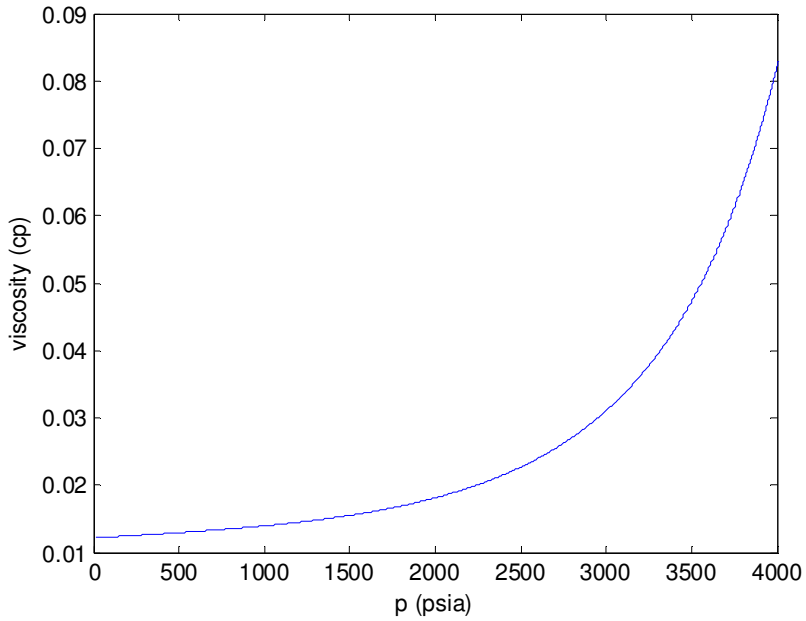

Figure 3-2: Plot of gas viscosity vs. pressure, applied to all the cases in this study.

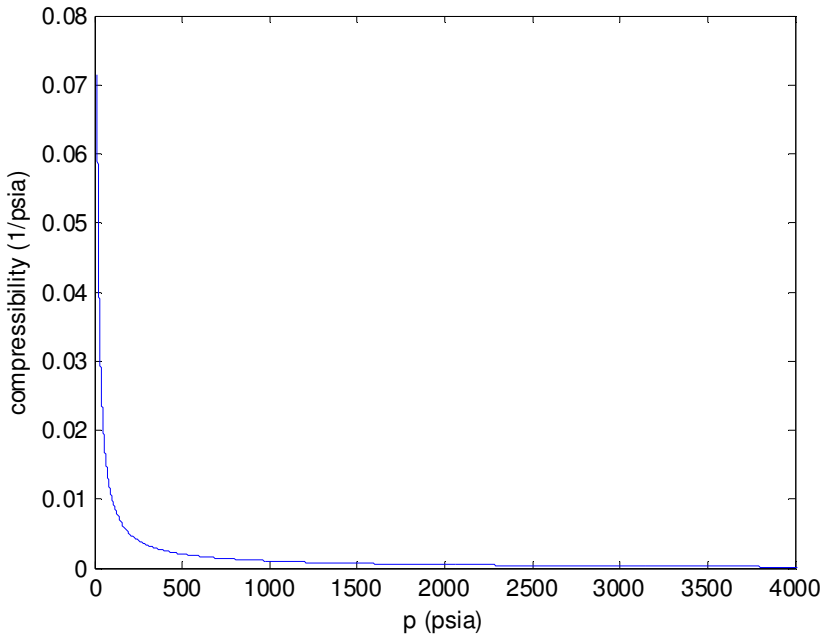

Figure 3-3: Plot of gas compressibility vs. pressure, applied to all the cases in this study.

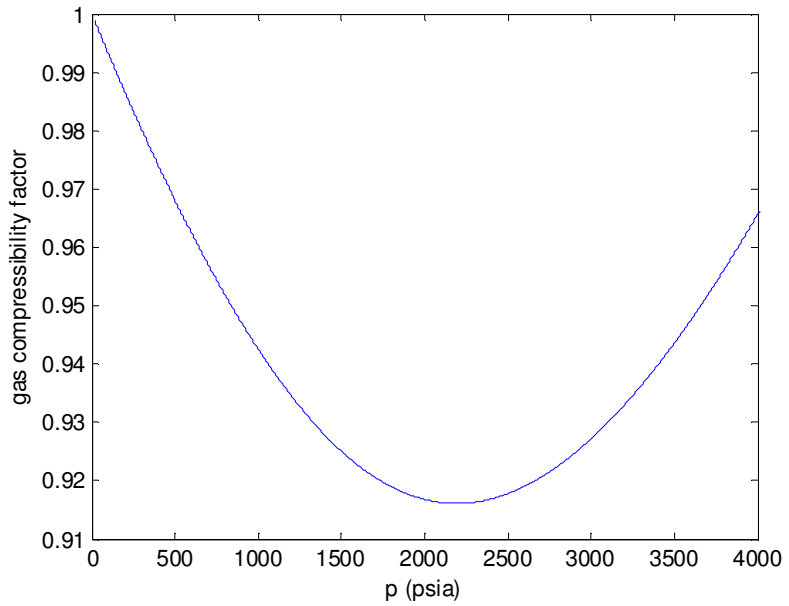

Figure 3-4: Plot of gas compressibility factor vs. pressure, applied to all the cases in this study.

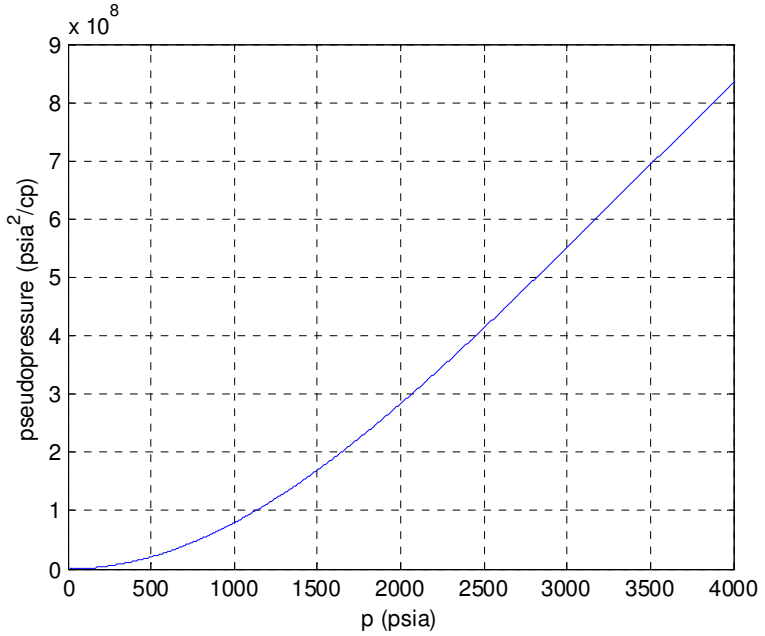

Figure 3-5: Plot pseudopressure vs. real pressure, applied to all the cases in this study.

3.2. Preview of the Case Studies

The objective of this study was to investigate the applicability of the pseudopressure, pseudotime, and material balance pseudotime methods by comparing the results of these methods with the Eclipse "data". Several cases were designed to study under which specific conditions these methods work or not.

Taking a look at the gas pseudotime Equation (2.17), which is rewritten as in Equation (3.1), we can find that the real time t is replaced by pseudotime t_a.

$$\frac{1}{r}\frac{\partial}{\partial r}(r\frac{\partial \varphi}{\partial r}) = \frac{\phi}{k}\frac{\partial \varphi}{\partial t_a} \tag{3.1}$$

When Equation (3.1) was solved, t_a took the place of t as the time variable on the right hand side of diffusion equation. Traditionally, t_a was considered to be a function of only t. However, as defined in Equation (2.16), t_a is also a function of the reservoir radius r, since μc is a function of reservoir pressure p and p is a function of r. Hence the actual form of the real gas flow equation in term of pseudotime is:

$$\frac{1}{r}\frac{\partial}{\partial r}(r\frac{\partial \varphi}{\partial r}) = \frac{\phi}{k}\frac{\partial \varphi}{\partial t_a(t,r)} \tag{3.2}$$

The term on the right hand side of Equation (3.2) is a differential of pseudopressure over pseudotime. Hence, the right hand side is a function of t and r. In practice, Equation (3.2) is solved as a traditional linear diffusion equation for liquid flow, which requires that the right hand side of the equation should be only deferential over time. The diffusion equation of liquid flow is shown in Equation (3.3):

$$\frac{1}{r}\frac{\partial}{\partial r}(r\frac{\partial \varphi}{\partial r}) = \frac{\phi}{k}\frac{\partial \varphi}{\partial t} \tag{3.3}$$

The true pseudotime equation is Equation (3.2). However, it is Equation (3.1) that was actually solved in the pseudotime method. Hence the solutions obtained from Equation (3.1) will not be completely valid. As defined in Equation (2.16), there is a relationship between t_a and r. Solving Equation (3.1) as a traditional linear diffusion equation directly will omit this connection between t_a and r.

Based on these discussions, it is reasonable to expect that the pressure drop over the reservoir radius r could influence the accuracy of pseudotime method. Specifically, the μc change over r could be a factor that determines the validity of the pseudotime method.

To verify this expectation, four drawdown cases were designed. Among these four cases, two of them were with a relatively high initial reservoir pressure, and the other two were with a relatively low initial reservoir pressure. For both the high initial pressure cases and the low initial pressure cases, the μc term was studied both as a strong function and a weak function of r. A brief description of the four cases is shown in Table 3-2. q is the gas production rate. Wellbore storage effect was not considered in this study.

In all the four cases the reservoir was considered to be closed boundary circular reservoir with $r_e = 500\,ft$. The well was at the center of the reservoir with $r_w = 3\,ft$.

To illustrate how strong or weak μc is as a function of r, we plot the changes of μc with r in Figure 3-6 and Figure 3-7. Figure 3-6 shows Case 1 and Case 2, which are the high initial reservoir pressure cases. Figure 3-7 shows Case 3 and Case 4, which are the low initial reservoir pressure cases. It should be noted that the curves in Figure 3-6 and Figure 3-7 are not μc, but the change of μc, which is defined as the ratio of the μc value at some reservoir radius r to the μc value at r_e. Both these curves were obtained when the average reservoir pressure dropped to around half of the initial reservoir pressure. In the "strong" μc cases, μc changed significantly along r. In the "weak" μc cases, μc changed only a little.

It should be noted that the four cases listed in Table 3-2 were not only designed for pressure drawdown tests, but were also applied to the drawdown-buildup test that is discussed in Section 3.4 and Section 3.5. The same parameters in Table 3-2 were applied except that the gas production rate q became zero after the well was shut in.

Table 3-2: Brief description of the four cases.

	Initial Pressure	μc as a function of r	Detailed information
Case 1	High	Strong	pi = 4000psia k = 3.3333md q = 10MMscf
Case 2	High	Weak	pi = 4000psia k = 33.3333md q = 1MMscf
Case 3	Low	Strong	pi = 900psia k = 33.3333md q = 3MMscf
Case 4	Low	Weak	pi = 900psia k = 33.3333md q = 0.1MMscf

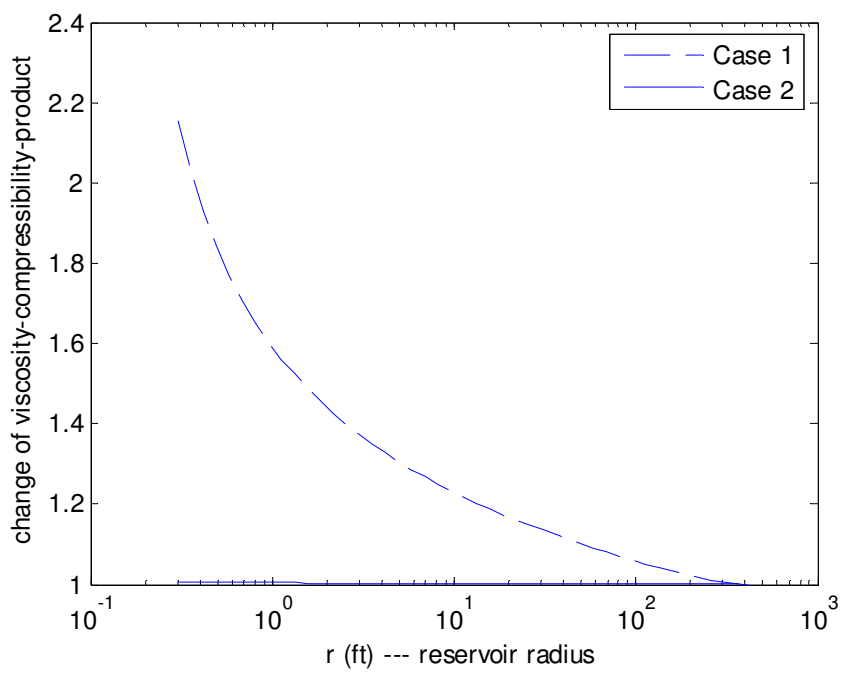

Figure 3-6: Change of μc as a function of the reservoir radius r for the high initial reservoir pressure Case 1 and Case 2. The μc curve was obtained when the average reservoir pressure dropped to around half of the initial reservoir pressure.

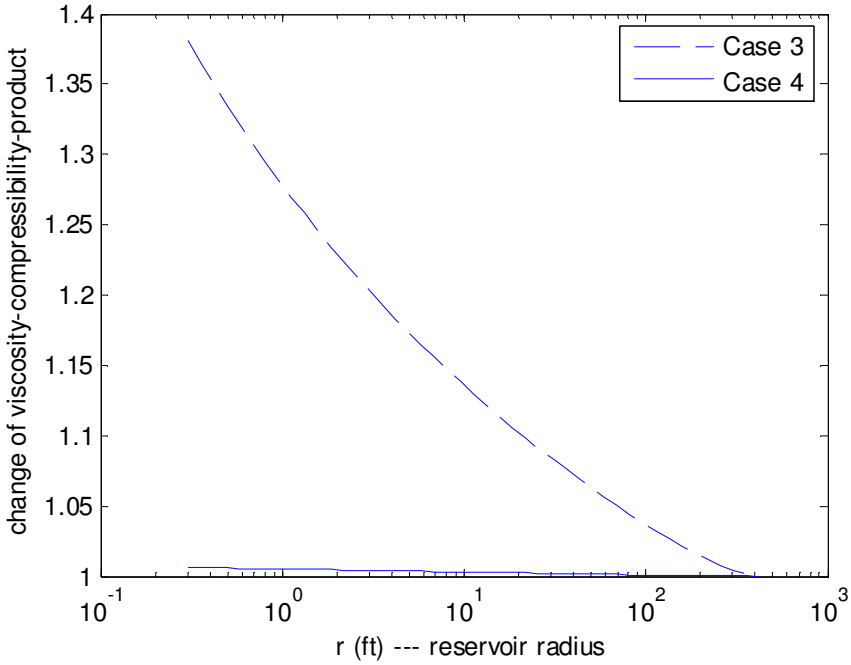

Figure 3-7: Change of μc as a function of the reservoir radius r for the low initial reservoir pressure Case 3 and Case 4. The μc curve was obtained when the average reservoir pressure dropped to around half of the initial reservoir pressure.

3.3. Drawdown Test During Pseudosteady State

This section presents the results of the four cases for a pressure drawdown test. Section 3.3.1 presents the discussion of the pseudotime method and Section 3.3.2 the material balance pseudotime method.

3.3.1. Discussion of the pseudotime method

The result of Case 1 is plotted in Figure 3-8 and Figure 3-9. Figure 3-8 shows the history plot of $\Delta p - t$. Figure 3-9 shows the log-log plot and derivative plot. In both figures the results of the pseudopressure method, the pseudotime method and the Eclipse "data" are plotted. There is a big deviation between the pseudotime method and the Eclipse "data". This suggests that the pseudotime method does not match when μc is a strong function of r for the case in which the initial reservoir pressure is relatively high.

The result of Case 2 is shown in Figure 3-10 and Figure 3-11 and is different from Case 1. The pseudotime method matches the Eclipse "data" very well even though the pseudopressure result deviates from the Eclipse "data" significantly. The difference between Case 1 and Case 2 is that μc is a strong function of r for Case 1, but a weak function of r for Case 2. Making a comparison between the results of Case 1 and Case 2, a temporary conclusion can be drawn: the pseudotime method is accurate if μc is a weak function of r, and inaccurate when μc is a strong function of.

After studying the high initial pressure Case 1 and Case 2, it is reasonable to have a look at the low initial pressure Case 3 and Case 4. The result of Case 3 is shown in Figure 3-12 and Figure 3-13 and is similar to that of Case 1. In both cases the pseudotime method does not match the Eclipse "data", and both Case 1 and Case 3 have strong μc as a function of r.

The result of Case 4 is plotted in Figure 3-14 and Figure 3-15. It is not surprising to see that the pseudotime method in Case 4 matches the Eclipse "data", since μc is a weak function of r.

The results of Case 3 and Case 4 not only confirm the temporary conclusion that the dependence of μc on r will influence the accuracy of pseudotime method, but also imply that the magnitude of the initial reservoir pressure is not a factor that determines whether pseudotime method is accurate or not.

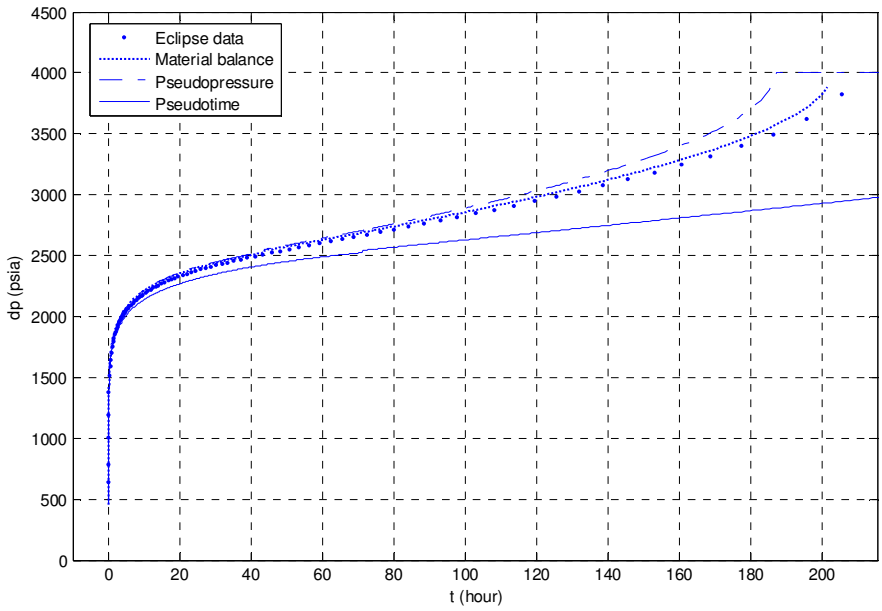

Figure 3-8: History plot of Case 1 with pressure drawdown to pseudosteady state.

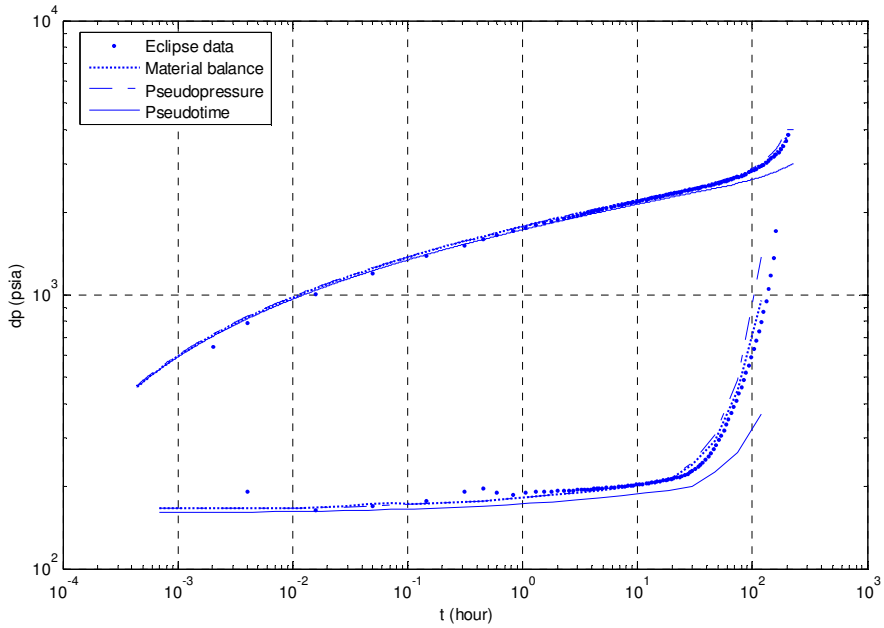

Figure 3-9: Log-log plot and derivative plot of Case 1 with pressure drawdown to pseudosteady state.

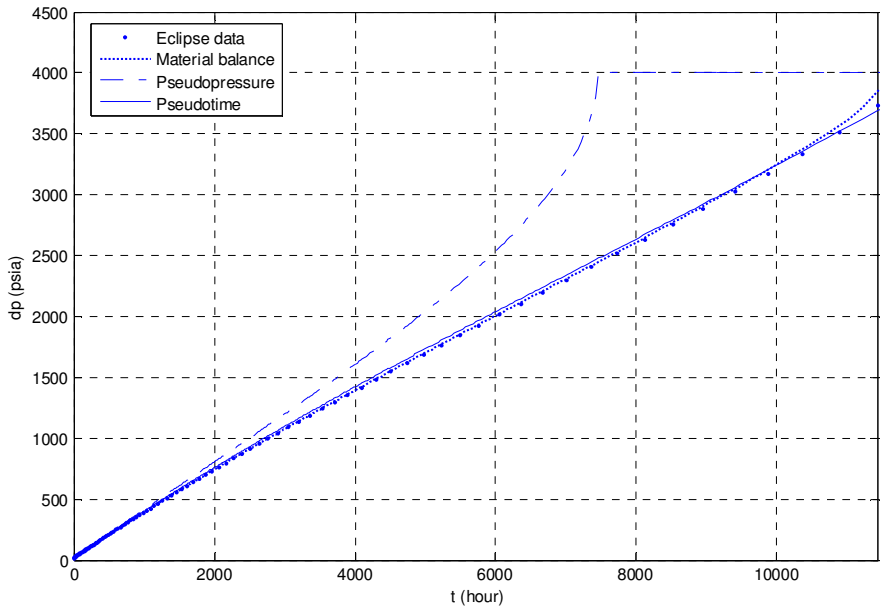

Figure 3-10: History plot of Case 2 with pressure drawdown to pseudosteady state.

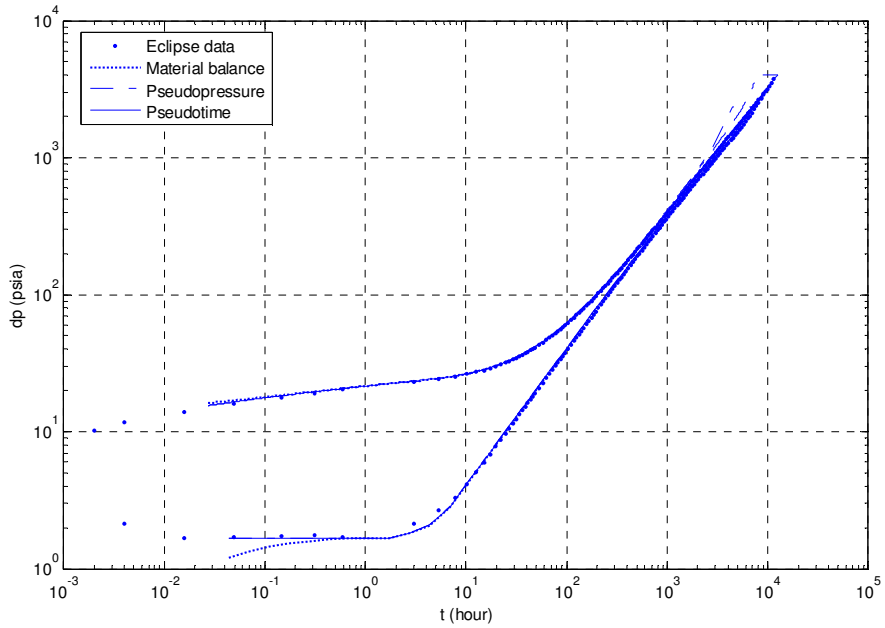

Figure 3-11: Log-log plot and derivative plot of Case 2 with pressure drawdown to pseudosteady state.

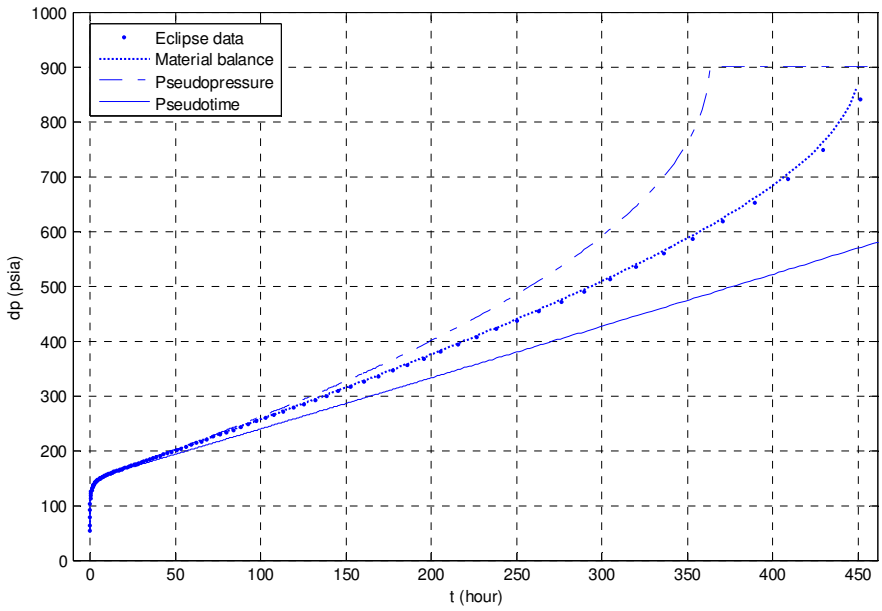

Figure 3-12: History plot of Case 3 with pressure drawdown to pseudosteady state.

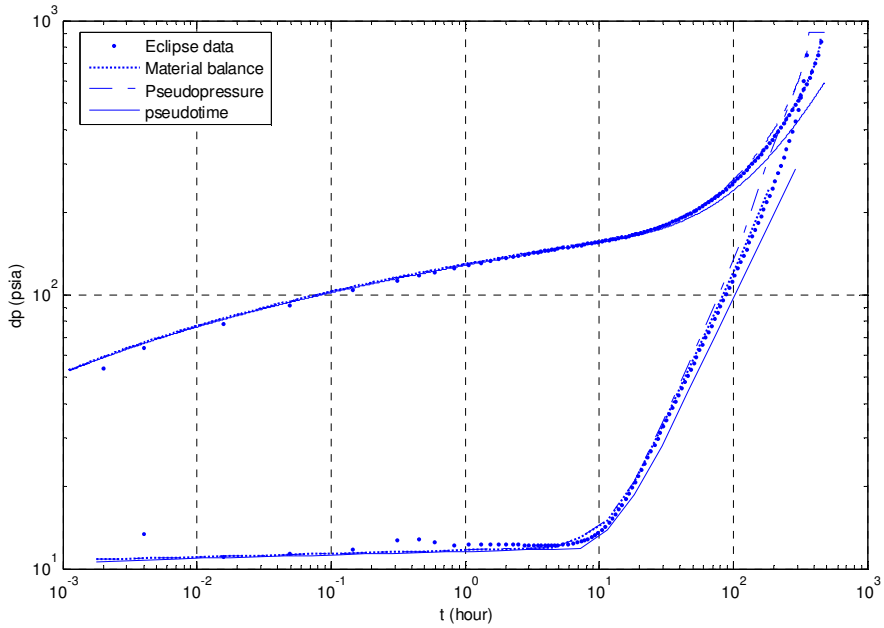

Figure 3-13: Log-log plot and derivative plot of Case 3 with pressure drawdown to pseudosteady state.

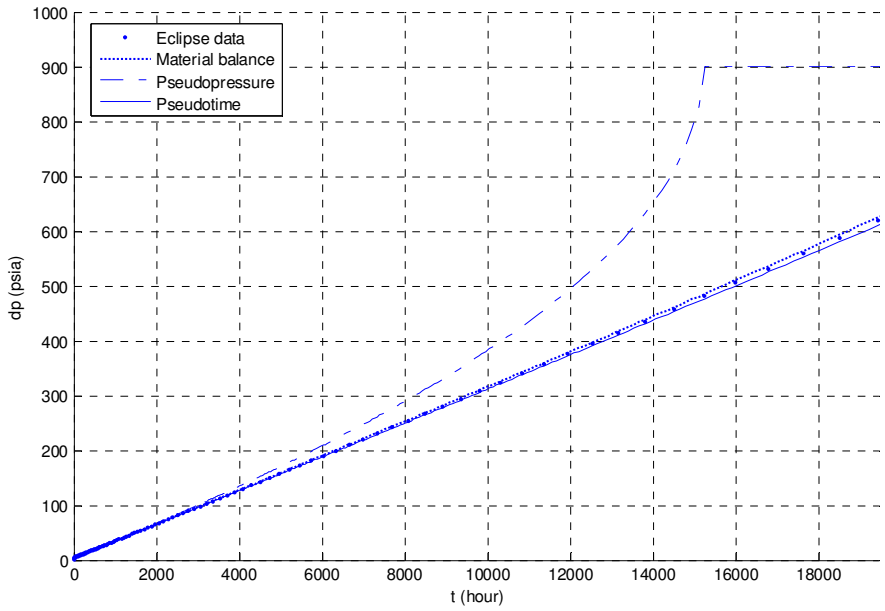

Figure 3-14: History plot of Case 4 with pressure drawdown to pseudosteady state.

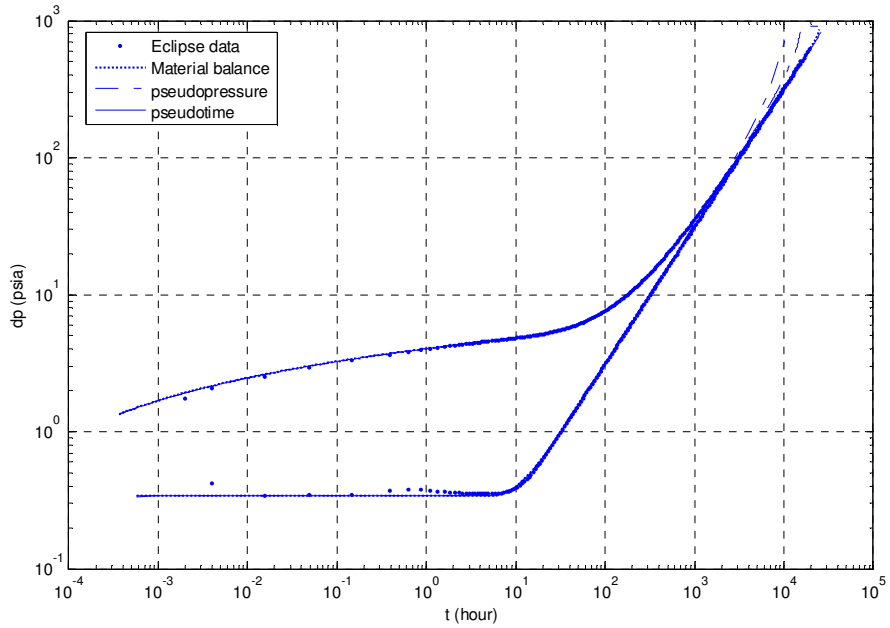

Figure 3-15: Log-log plot and derivative plot of Case 4 with pressure drawdown to pseudosteady state.

3.3.2. Discussion of the material balance pseudotime method

The results of material balance pseudotime method are plotted in dotted lines in Figures 3-8 to 3-15. Since the material balance pseudotime method is a variation of the pseudotime method, it is reasonable to assume that the material balance pseudotime method also works when the pseudotime method is accurate. This assumption was confirmed by applying the material balance pseudotime method to Case 2 and Case 4. In Figure 3-10 and Figure 3-14, which are the history plots of Case 2 and Case 4, the material balance pseudotime method matches the Eclipse "data".

Figure 3-8 and Figure 3-12 show the history plots of Case 1 and Case 3. The pseudotime method does not work in these two cases, but the material balance pseudotime method matches the Eclipse "data" much better than the pseudotime method. Although the match is not perfect, it improves significantly. The error will become acceptable if the change of μc is more moderate. Based on these observations, another conclusion can be drawn: the material balance pseudotime method can improve the accuracy of the pseudotime method significantly, but not fully.

It is interesting to compare the results of the material balance method between Case 1 and Case 3. The material balance method matches the Eclipse "data" in Case 3 better than in Case 1. To find the reason, we should review the plots of the change of μc over the reservoir radius r, as shown in Figure 3-6 and Figure 3-7. The dashed lines in Figure 3-6 and Figure 3-7 are for Case 1 and Case 3 respectively. The μc term in Case 1 changes much more than in Case 3 and has a stronger dependence on r than in Case 3. These suggest that, the more μc changes as a function r, the less the material balance pseudotime method matches the Eclipse "data".

3.4. Buildup During Infinite-Acting Radial Flow Period

In Section 3.4 and Section 3.5 the results of buildup tests are presented. In the buildup cases used in this section, the producing well was shut in at the end of the infinite-acting radial flow period. In Section 3.5, the well was shut in during pseudosteady state. The same parameters used in Section 3.3 were applied in Section 3.4.

The results of Cases 1, 2, 3 and 4 are shown in Figures 3-16 to 3-27. For each case, the log-log plot, log-log and derivative plot and history plot are drawn.

Since the well was shut in at the end of the infinite-acting radial flow period, the average reservoir pressure did not drop significantly, and the accumulated error that occurred in the pseudotime-related calculation was small.

For Case 2 and Case 4, the results of the three analytical methods match each other very well, even though they do not have a perfect match with the Eclipse "data". One conclusion can be drawn based on the results of Case 2 and Case 4: as μc is a weak function of r, the pseudopressure, pseudotime and material balance pseudotime methods are almost identical to each other during the infinite-acting radial flow.

For Case 1 and Case 3, in which μc is a strong function of r, these three methods do not show the same extent of agreement as in Case 2 and Case 4. However, in these two cases the pseudopressure method and the material balance pseudotime method have a good match to each other. This observation suggests that the material balance pseudotime method is identical to the pseudopressure method if the shut-in time is short.

Since the predictions of these three methods are really close, it is hard to determine which method is better or has less error due to the incomplete time superposition.

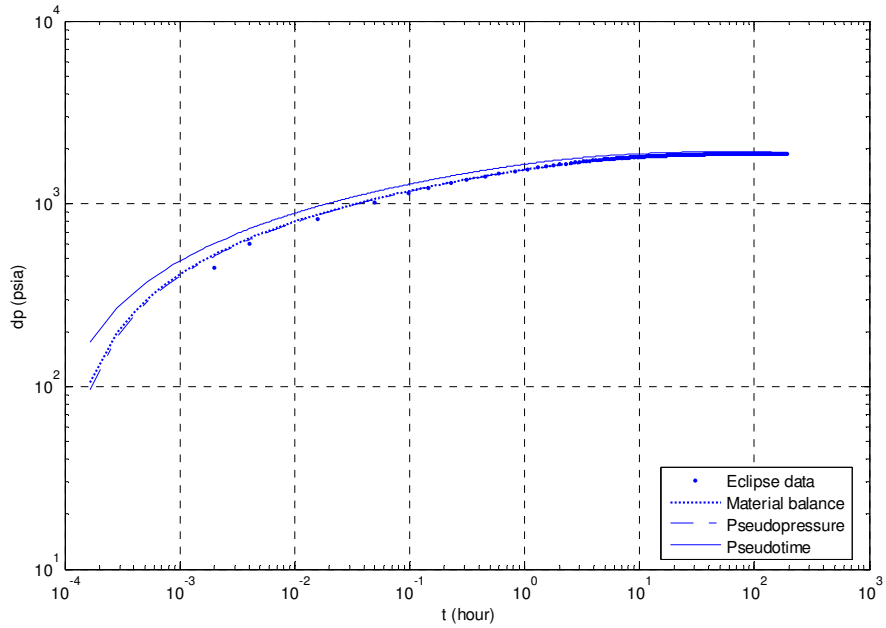

Figure 3-16: Log-log plot of Case 1 with buildup at the end of infinite-acting radial flow period.

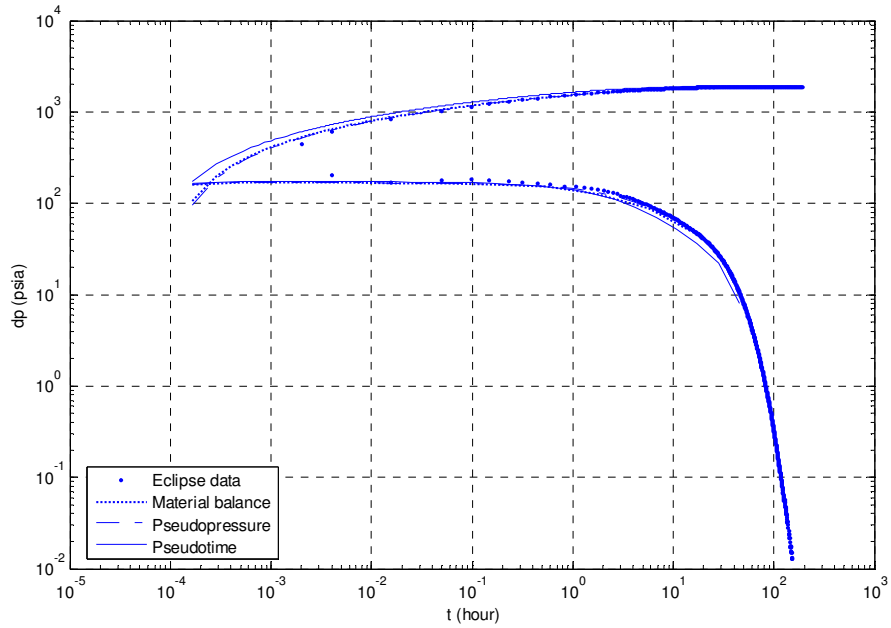

Figure 3-17: Log-log plot and derivative plot of Case 1 with buildup at the end of infinite-acting radial flow period.

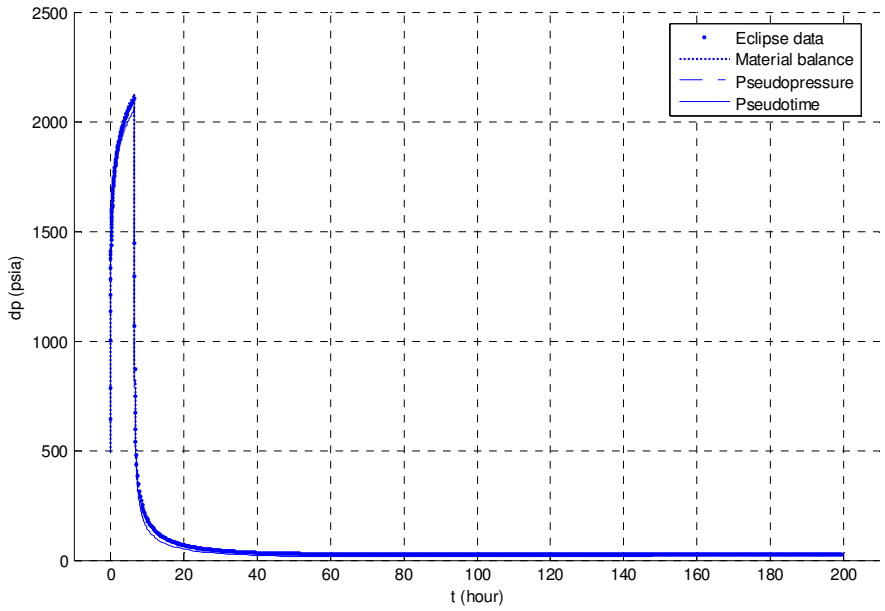

Figure 3-18: History plot of Case 1 with buildup at the end of infinite-acting radial flow period.

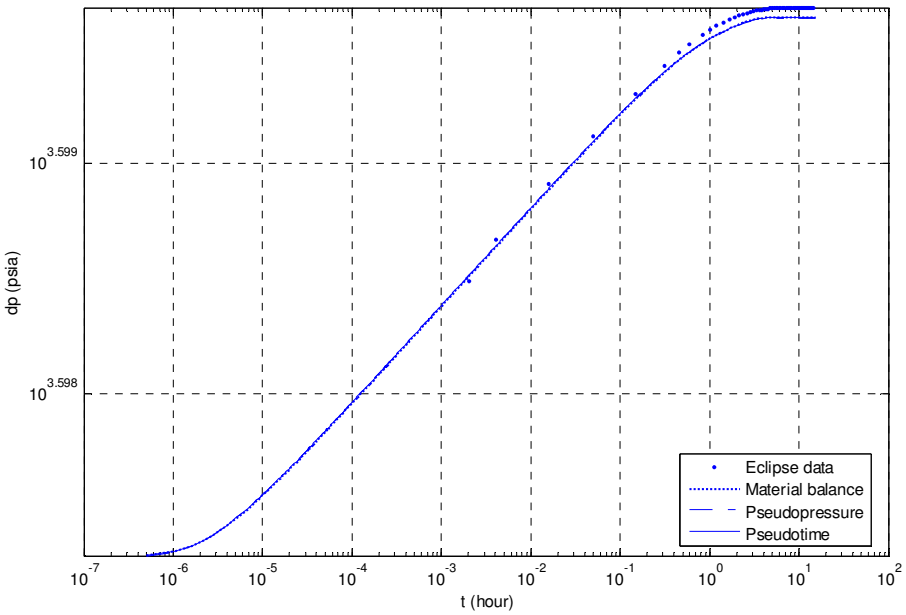

Figure 3-19: Log-log plot of Case 2 with buildup at the end of infinite-acting radial flow period.

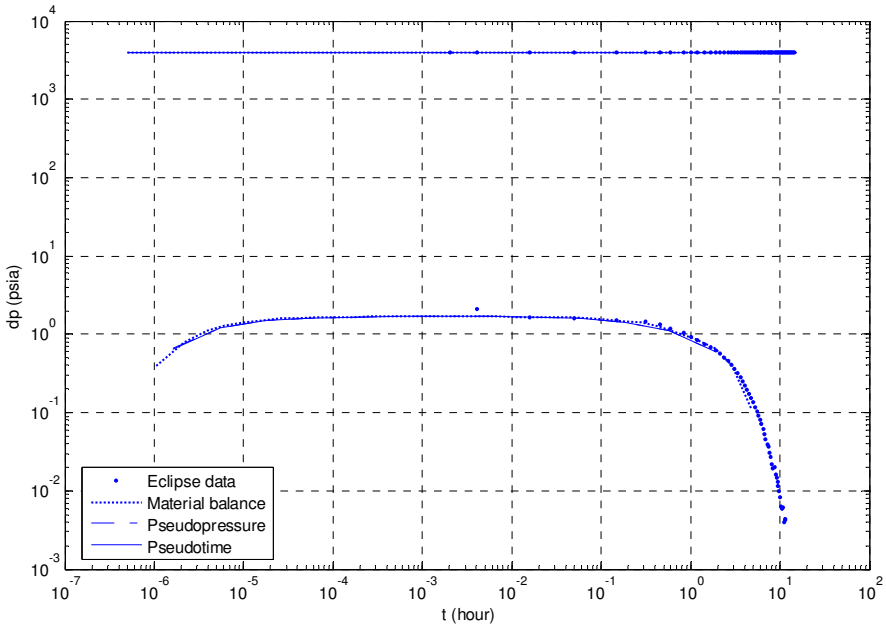

Figure 3-20: Log-log plot and derivative plot of Case 2 with buildup at the end of infinite-acting radial flow period.

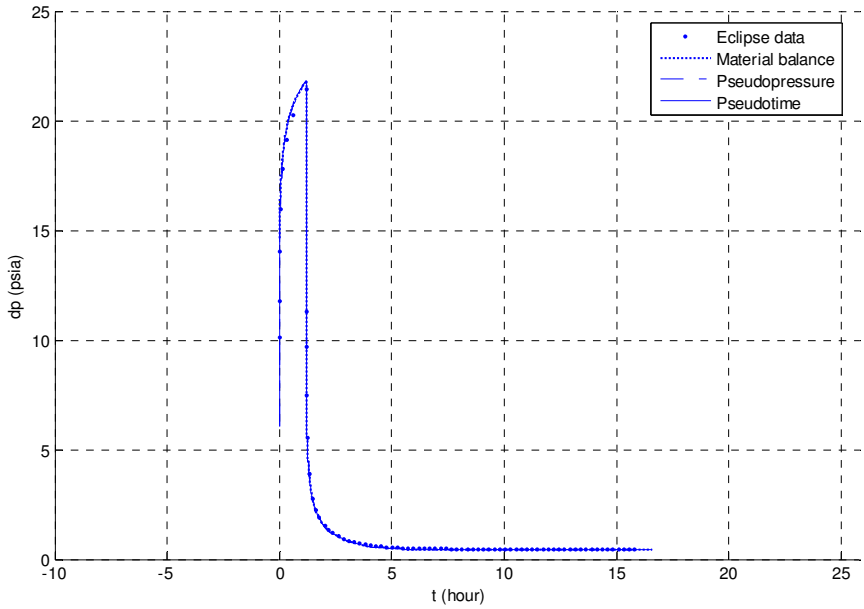

Figure 3-21: History plot of Case 2 with buildup at the end of infinite-acting radial flow period.

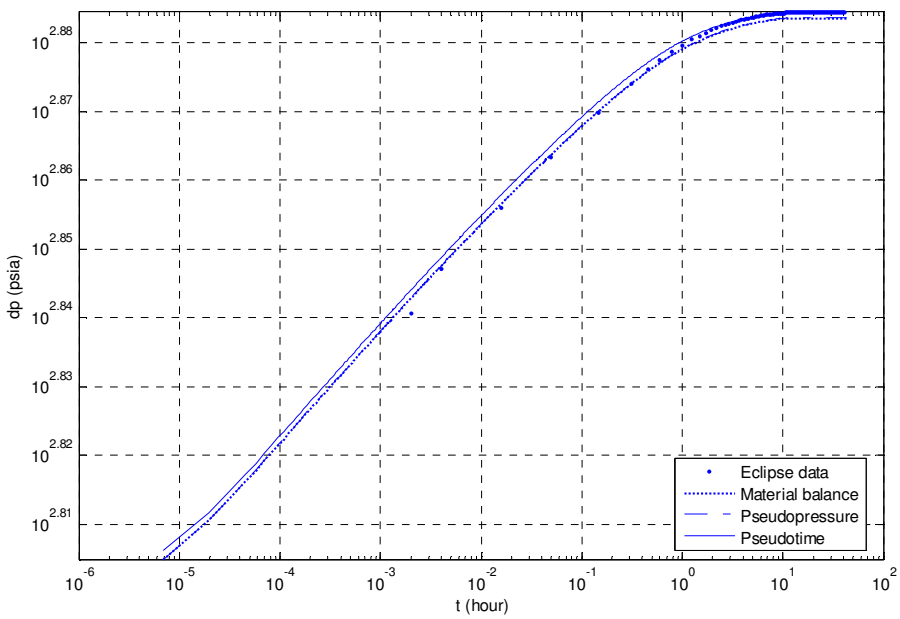

Figure 3-22: Log-log plot of Case 3 with buildup at the end of infinite-acting radial flow period.

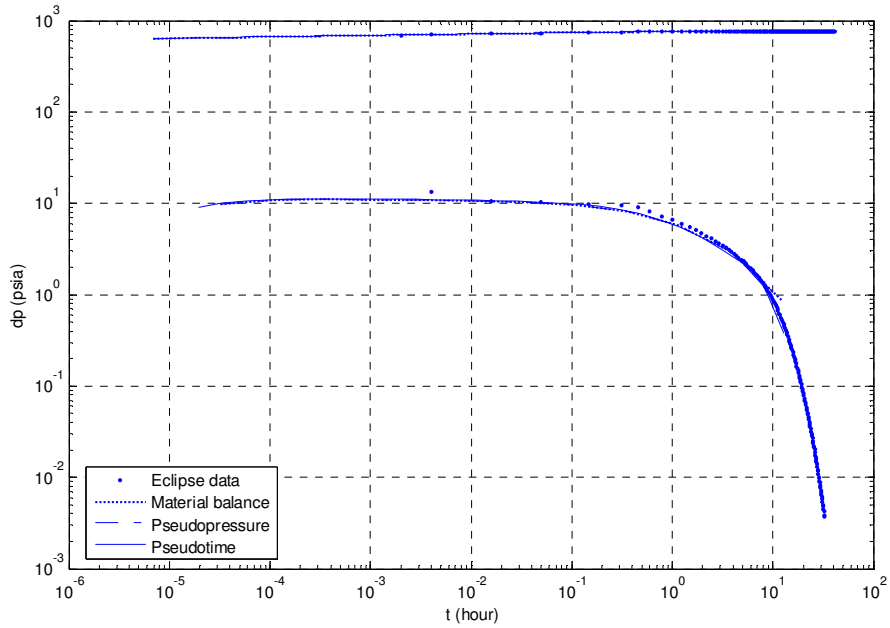

Figure 3-23: Log-log plot and derivative plot of Case 3 with buildup at the end of infinite-acting radial flow period.

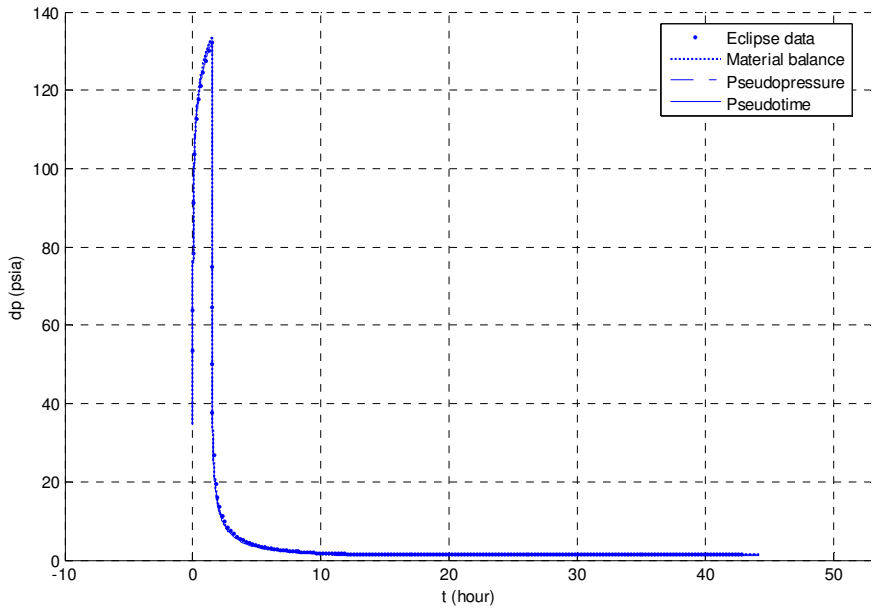

Figure 3-24: History plot of Case 3 with buildup at the end of infinite-acting radial flow period.

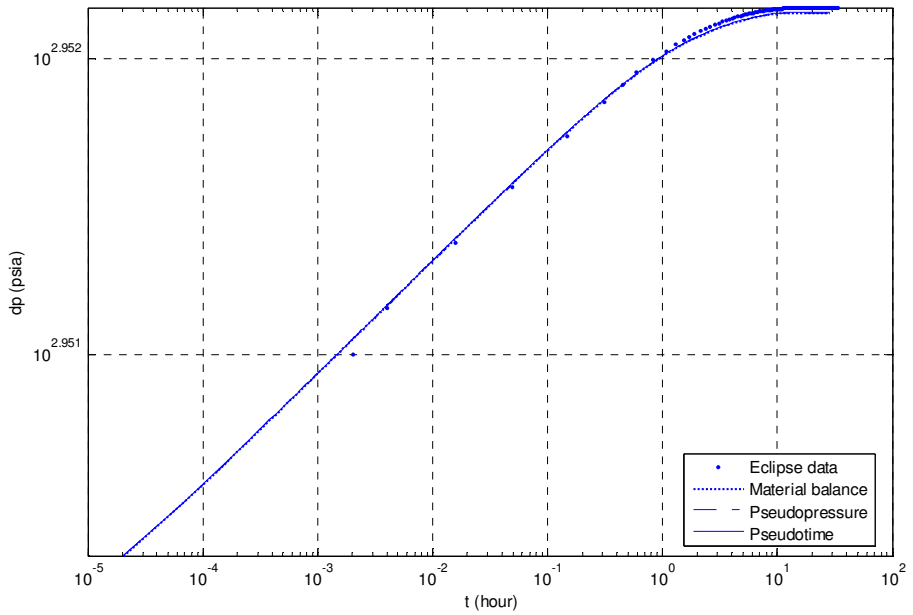

Figure 3-25: Log-log plot of Case 4 with buildup at the end of infinite-acting radial flow period.

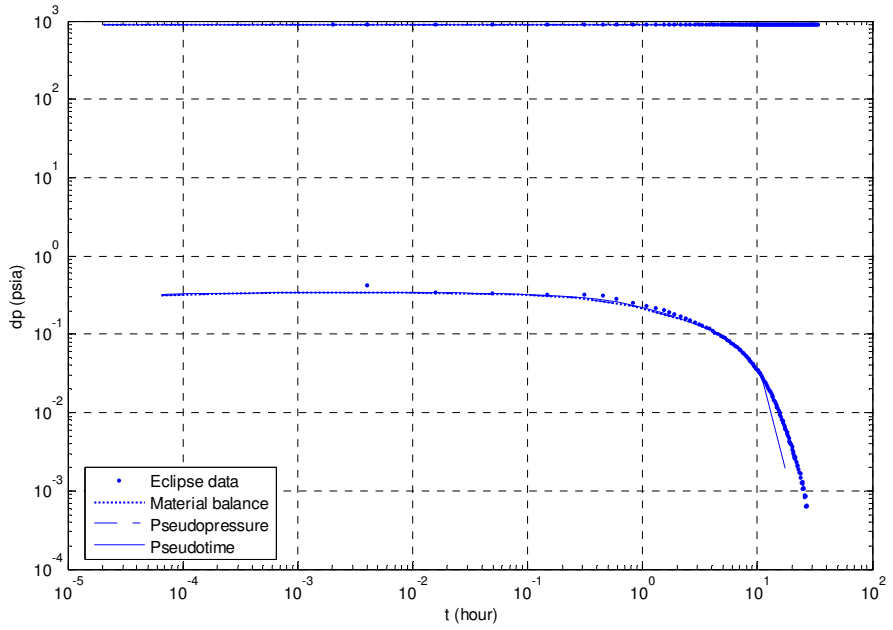

Figure 3-26: Log-log plot and derivative plot of Case 4 with buildup at the end of infinite-acting radial flow period.

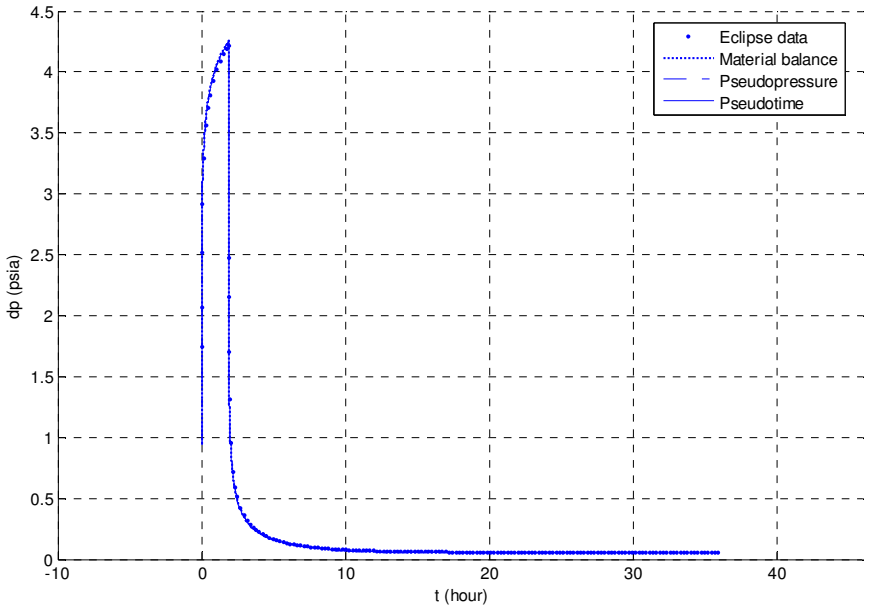

Figure 3-27: History plot of Case 4 with buildup at the end of infinite-acting radial flow period.

3.5. Buildup During Pseudosteady State

In this section the effect of late buildup is studied. The producing well was shut in when the average reservoir pressure dropped to around half of the initial reservoir pressure, which occurred during pseudosteady state.

The results of Case 1 to Case 4 are presented in Figures 3-28 to 3-39. The log-log plot, log-log and derivative plot and history plot are drawn.

Figure 3-28 shows the log-log plot of Case 1. There is a big deviation between the result of the pseudotime method and the Eclipse "data". The deviation of the pseudotime method is much larger than that of the pseudopressure method. This observation is similar to that of the history plot in Case 1, which is shown in Figure 3-30. In Figure 3-30, the deviation of the pseudotime method during drawdown period is also much larger than that of the pseudopresssure method. This suggests that the accuracies of the pseudotime and pseudopressure methods during the drawdown period determine the accuracies of these two methods during the buildup period. It also means that, although the time superposition in the pseudopressure method is incomplete compared to the pseudotime method, the error is acceptable.

By looking at the other three cases, similar observations can be made and the following conclusion can be drawn. During the late buildup, the incomplete time superposition does not influence the accuracies of the pseudopressure method greatly. The accuracies of the pseudopressure and pseudotime methods during the drawdown period influence their accuracies during the buildup period significantly.

However, this conclusion may not be applied to the material balance pseudotime method. In Figure 3-36, which shows the history plot of Case 3, the material balance pseudotime method matches the Eclipse "data" much better than the pseudotime method. If the previous conclusion applies to the material balance pseudotime method, the log-log plot of the material balance pseudotime method should also match the Eclipse "data" much better than that of the pseudotime method. However, in the log-log plot of Case 3 (Figure

3-34), there is a big deviation between the material balance pseudotime method and the Eclipse "data". This deviation is almost as large as that of the pseudotime method.

In the history plot of Case 4 (Figure 3-39), the material balance pseudotime method matches the Eclipse "data" better than the pseudotime method. But in the log-log plot of Case 4 (Figure 3-37), the result of material balance pseudotime method is even worse than that of the pseudotime method. This is not consistent with the conclusion for the pseudopressure and pseudotime methods that was drawn previously in this section.

Both Case 3 and Case 4 are low initial pressure cases. In these two cases, μc as a function of r is relatively weaker than in Case 1 and Case 4. For the material balance pseudotime method, there is probably some relation between the error of the incomplete time superposition and the μc distribution along r. This should be investigated in the future work.

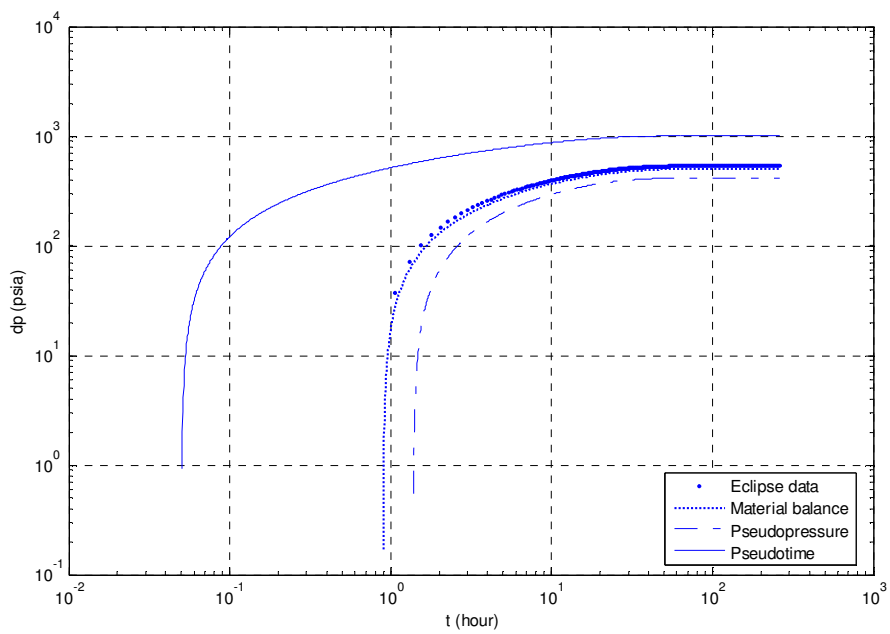

Figure 3-28: Log-log plot of Case 1 with buildup during pseudosteady state.

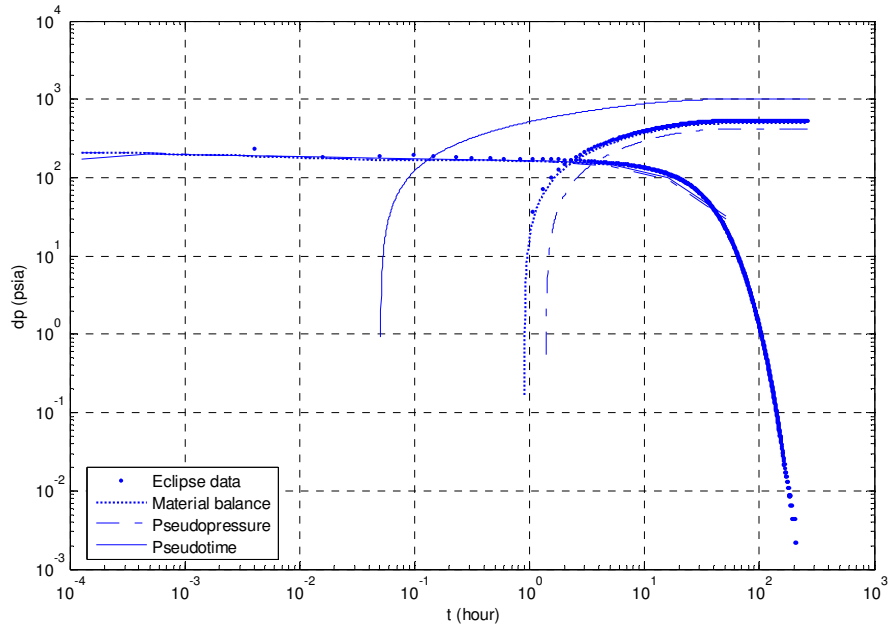

Figure 3-29: Log-log plot and derivative plot of Case 1 with buildup during pseudosteady state.

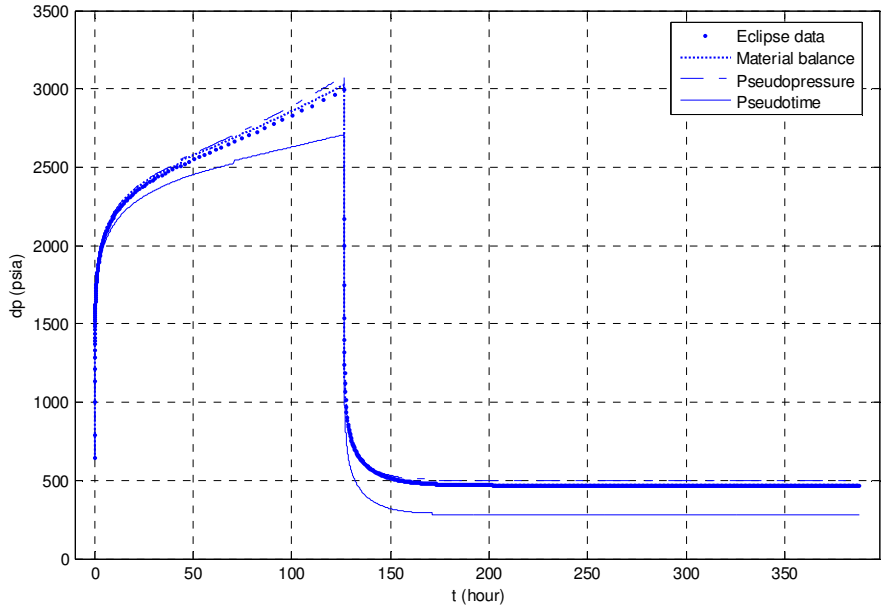

Figure 3-30: History plot of Case 1 with buildup during pseudosteady state.

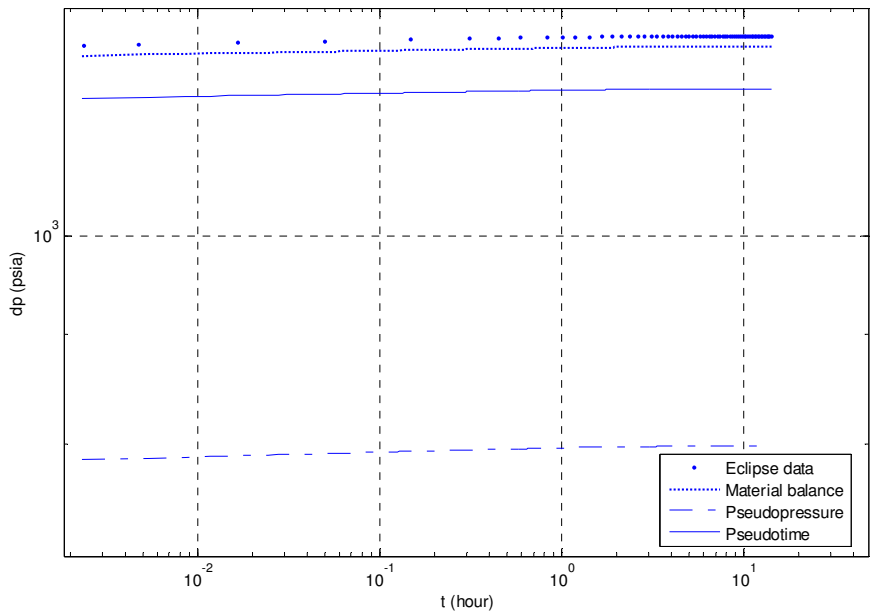

Figure 3-31: Log-log plot of Case 2 with buildup during pseudosteady state.

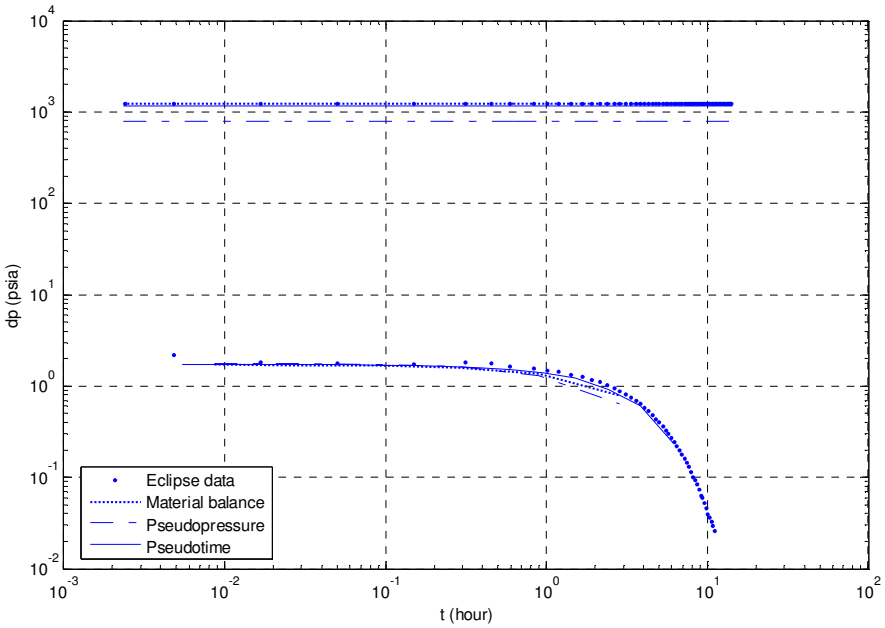

Figure 3-32: Log-log plot and derivative plot of Case 2 with buildup during pseudosteady state.

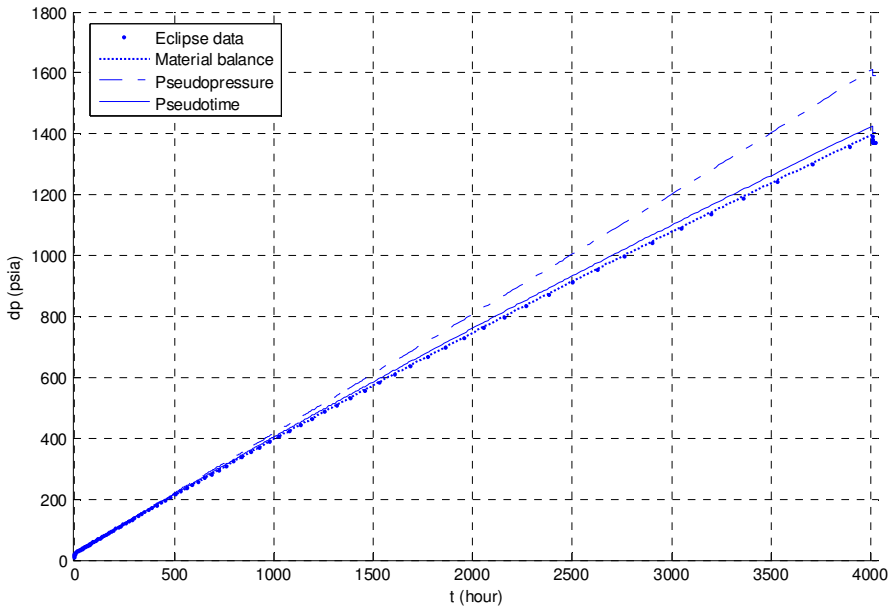

Figure 3-33: History plot of Case 2 with buildup during pseudosteady state.

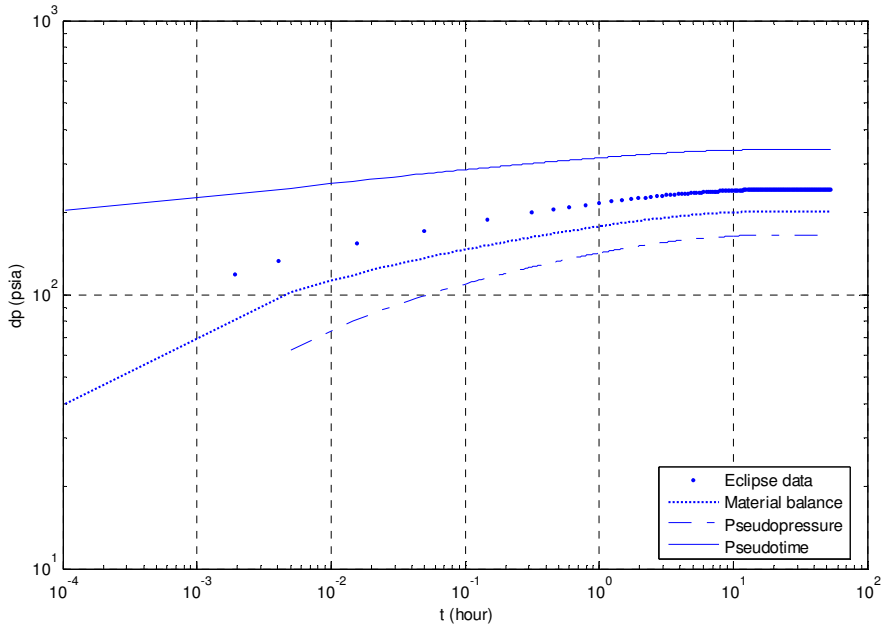

Figure 3-34: Log-log plot of Case 3 with buildup during pseudosteady state.

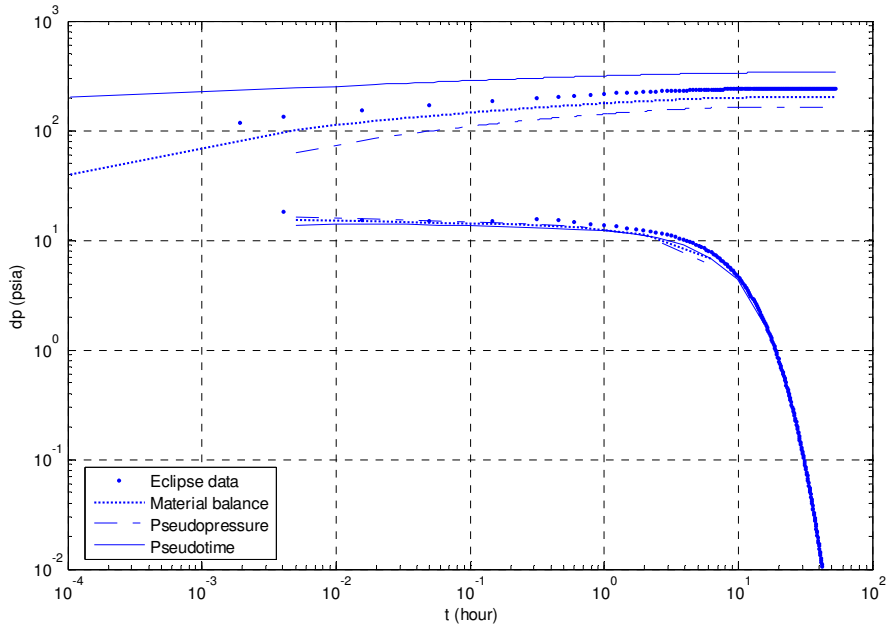

Figure 3-35: Log-log plot and derivative plot of Case 3 with buildup during pseudosteady state.

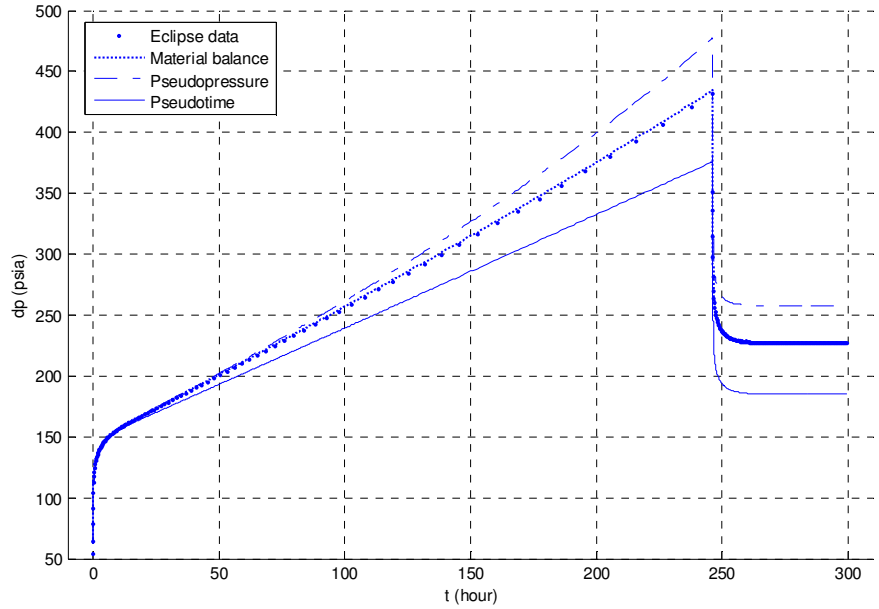

Figure 3-36: History plot of Case 3 with buildup during pseudosteady state.

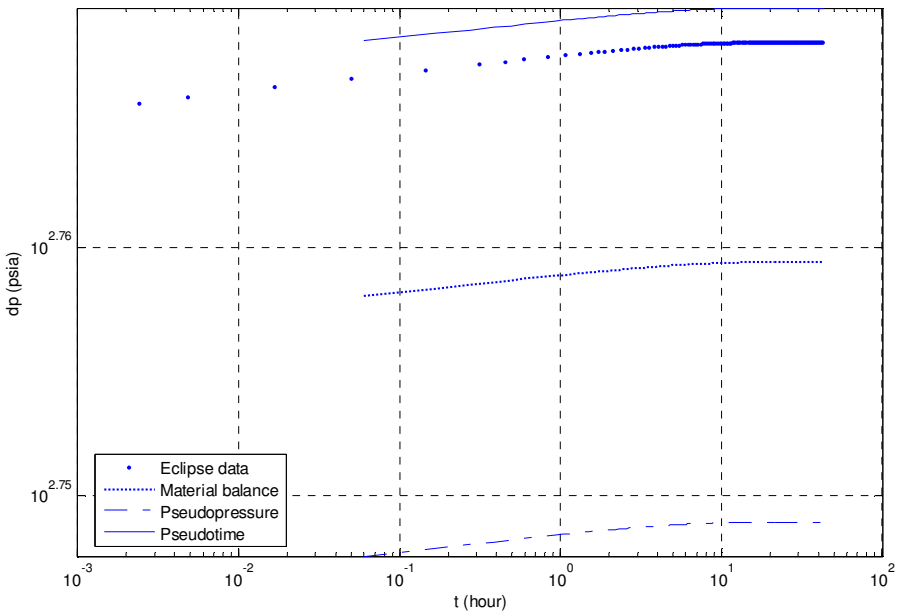

Figure 3-37: Log-log plot of Case 4 with buildup during pseudosteady state.

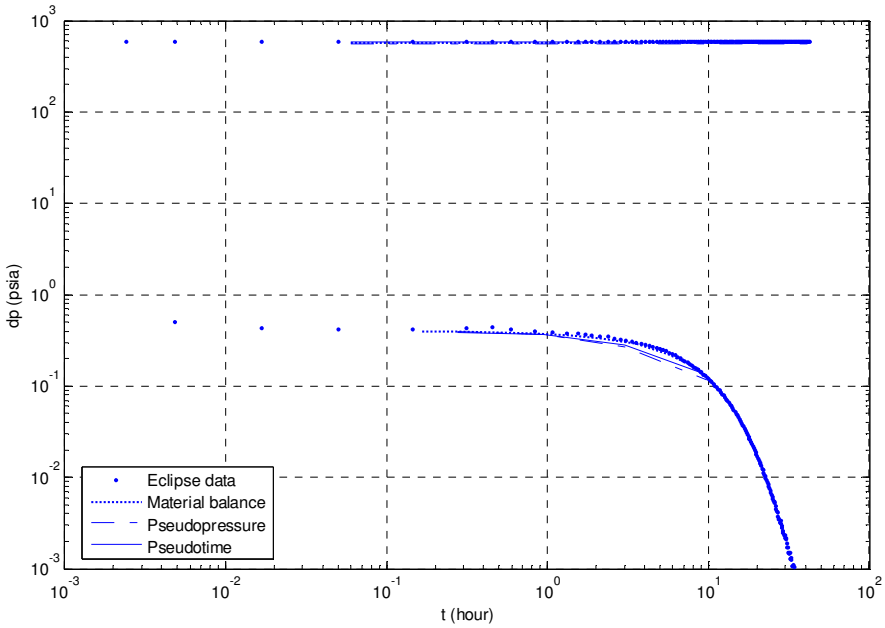

Figure 3-38: Log-log plot and derivative plot of Case 4 with buildup during pseudosteady state.

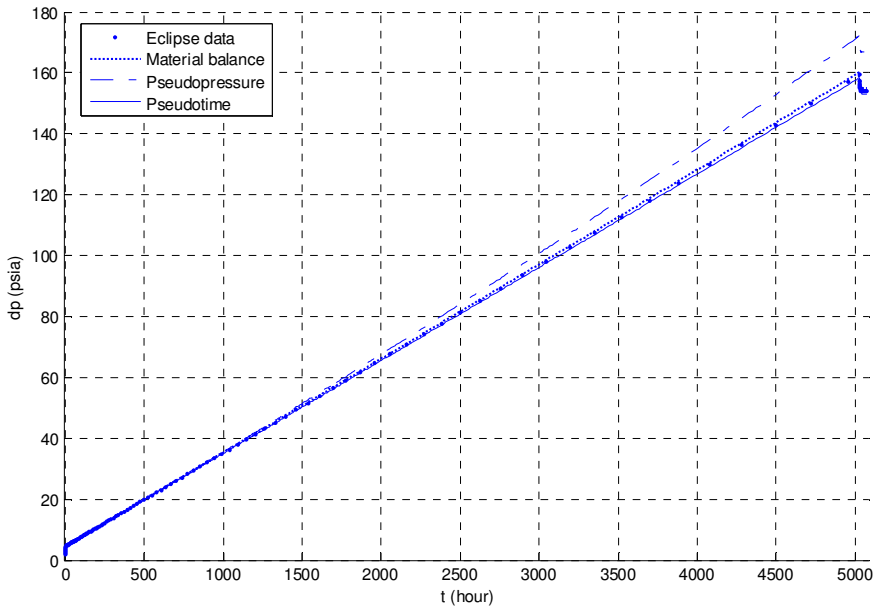

Figure 3-39: History plot of Case 4 with buildup during pseudosteady state.

Chapter 4

4. Conclusions

The objective of this study was to investigate the applicability of the pseudopressure, pseudotime and material balance pseudotime method with the assumption that "full physics" simulation data are accurate. Two-dimensional single-phase gas flow in a closed-boundary circular reservoir was studied. Several cases were designed and the results of these three analytical methods were compared with that of Eclipse simulations. The following conclusions were made on the basis of the results of the case studies:

a) The pseudotime method is accurate if the viscosity-compressibility factor μc is a weak function of the reservoir radius r, and is inaccurate if μc is a strong function.

b) The magnitude of the initial reservoir pressure is not a factor that influences the accuracy of pseudotime.

c) The material balance pseudotime method improves the accuracy of the pseudotime method significantly, but not fully.

d) For buildup tests with the well shut in during the infinite-acting radial flow period, the pseudopressure, pseudotime and material balance pseudotime methods are almost identical to each other if μc is a weak function of r.

e) For buildup tests with the well shut in during pseudosteady state, the incomplete time superposition of the pseudopressure method does not influence its accuracy significantly. The accuracies of the pseudopressure and pseudotime methods during drawdown period determine their accuracies during buildup period.

Besides these conclusions, some observations were also made:

a) For drawdown tests, the less μc changes as a function of r, the better the material balance pseudotime method matches the Eclipse "data".

b) For the buildup test with the well shut in during the infinite-acting radial flow period, the material balance pseudotime method is almost identical to the pseudopressure method.

Nomenclature

A = Reservoir area, ft

B_{gi} = Gas formation volume factor at p_i, cf/scf

c = Gas compressibility at p, psia^{-1}

c_i = Gas compressibility p_i, psia^{-1}

G = Original gas in place, MMscf

G_p = Cumulative gas production, MMscf

h = Pay thickness, ft

k = Reservoir permeability, md

M = Molecular weight, lb/lb-mole

p = Reservoir pressure, psia

p^o = Reference pressure, psia

$\overline{p}$ = Average reservoir pressure, psia

p_D = Dimensionless pressure

p_i = Initial reservoir pressure, psia

p_t = Dimensionless pressure drop at the well excluding skin effect

p_{wf} = Well flowing pressure, psia

Δp = Pressure drop at the well, psia

q = Gas production rate, MMscf/day

q_D = Dimensionless gas production rate

r = Radius, ft

r_D = Dimensionless radius

r_e = Reservoir radius, ft

r_w = Wellbore radius, ft

R = Gas constant, 10.7 ft^3-psia/lbmole-^oR

S_{wi} = Water saturation at p_i

t = Real time, hour

t_a = Pseudotime, hour-psi/cp

t_{aD} = Dimensionless pseudotime

t_p = Well shut-in time in buildup test, hour

t_{pD} = Dimensionless well shut-in time in buildup test, hour

t_{paD} = Dimensionless pseudotime correspoinding to t_p.

T = Temperature, ^oR

$\vec{u}$ = Velocity vector, ft/sec

z = Gas compressibility factor at p

$\bar{z}$ = Gas compressibility factor at $\bar{p}$

z_i = Gas compressibility factor at p_i

ρ = Fluid density, lb/ft^3

γ = Constant for field units, 1.422e6

λ = Constant for field units, 2.637e-4

μ = Gas viscosity at p, cp

μ_i = Gas viscosity at p_i, cp

ϕ = Porosity

φ = Pseudopressure corresponding to p, $psia^2$/cp

φ_i = Pseudopressure corresponding to p_i, $psia^2$/cp

φ_D = Dimensionless pseudopressure corresponding to p

References

Agarwal, R. G.: "Real Gas Pseudotime – A New Function for Pressure Buildup Analysis of Gas Wells", paper SPE 8279 presented at the 1979 SPE Annual Technical Conference and Exhibition, Las Vegas, Nevada, September 23-26, 1979.

Al-Hussainy, R. and Ramey, H. J. Jr.: "Application of Real Gas Flow Theory to Well Testing and Deliverability Forecasting", *J. Pet. Tech.* (May 1966) 637-642; Trans., AIME, 237.

Anisur Rahman, N. M., Mattar, L. and Zaoral, K.: "A New Method for Computing Pseudo-Time for Real Gas Flow Using the Material Balance Equation", paper 2004-182 presented at the Petroleum Society's 5th Canadian International Petroleum Conference (55th Annual Technical Meeting), Calgary, Alberta, Canada, June 8-10, 2004.

Energy Resources Conservation Board, Alberta, Canada: "Gas Well Testing: Theory and Practice", 4th edition, 1979.

Gardner, D. C., Hager, C. J. and Agarwal, R. G.: "Incorporating Rate-Time Superposition Into Decline Type Curve Analysis", paper SPE 62475 presented at the 2000 SPE Rocky Mountain Regional/Low Permeability Reservoir Symposium, Denver, Colorado, March 12-15, 2000.

Horne, R. N.: "Modern Well Test Analysis: A Computer-Aided Approach", (1995) 54-55, 207-211.

Lee, W. J. and Holditch, S. A.: "Application of Pseudotime to Buildup Test Analysis of Low Permeability Gas Wells with Long-Duration Wellbore Storage Distortion", *J. Pet. Tech.* (December 1982) 2877-2887.

Ramagost, B. P., Farshad, F. F.: "P/Z Abnormally Pressured Gas Reservoir", paper SPE 10125 presented at the 58th Annual Fall Technical Conference and Exhibition

of the Society of Petroleum Engineering of AIME, San Antonio, Texas, October 5-7, 1981.